HP2024
NAGASAKI

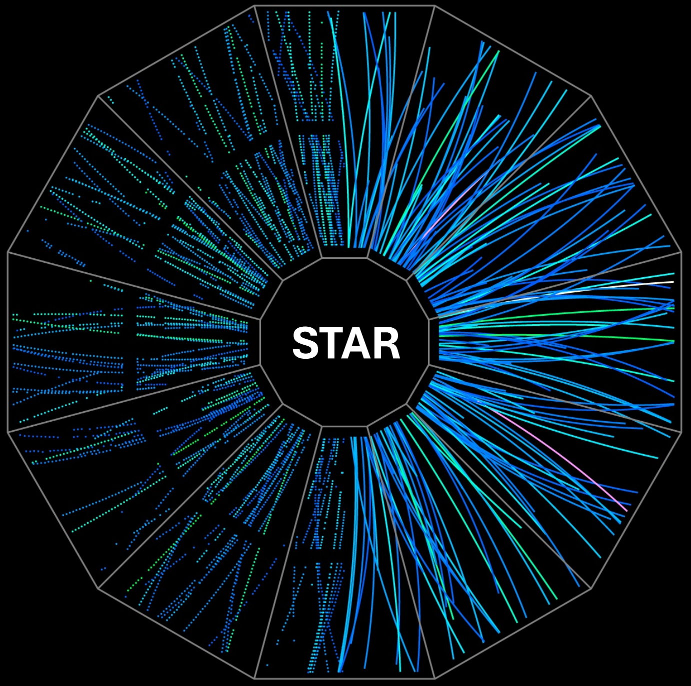


# Charm Meson Tagged Jets in Au + Au Collisions at $\sqrt{s_{NN}}$ = 200 GeV

**Diptanil Roy**
*(On behalf of the STAR Collaboration)*
*Rutgers University*
*roydiptanil@gmail.com*

*September 25, 2024*

RUTGERS
NSF
Supported in part by U.S. DEPARTMENT OF ENERGY | Office of Science

# Introduction

# Jets in HIC

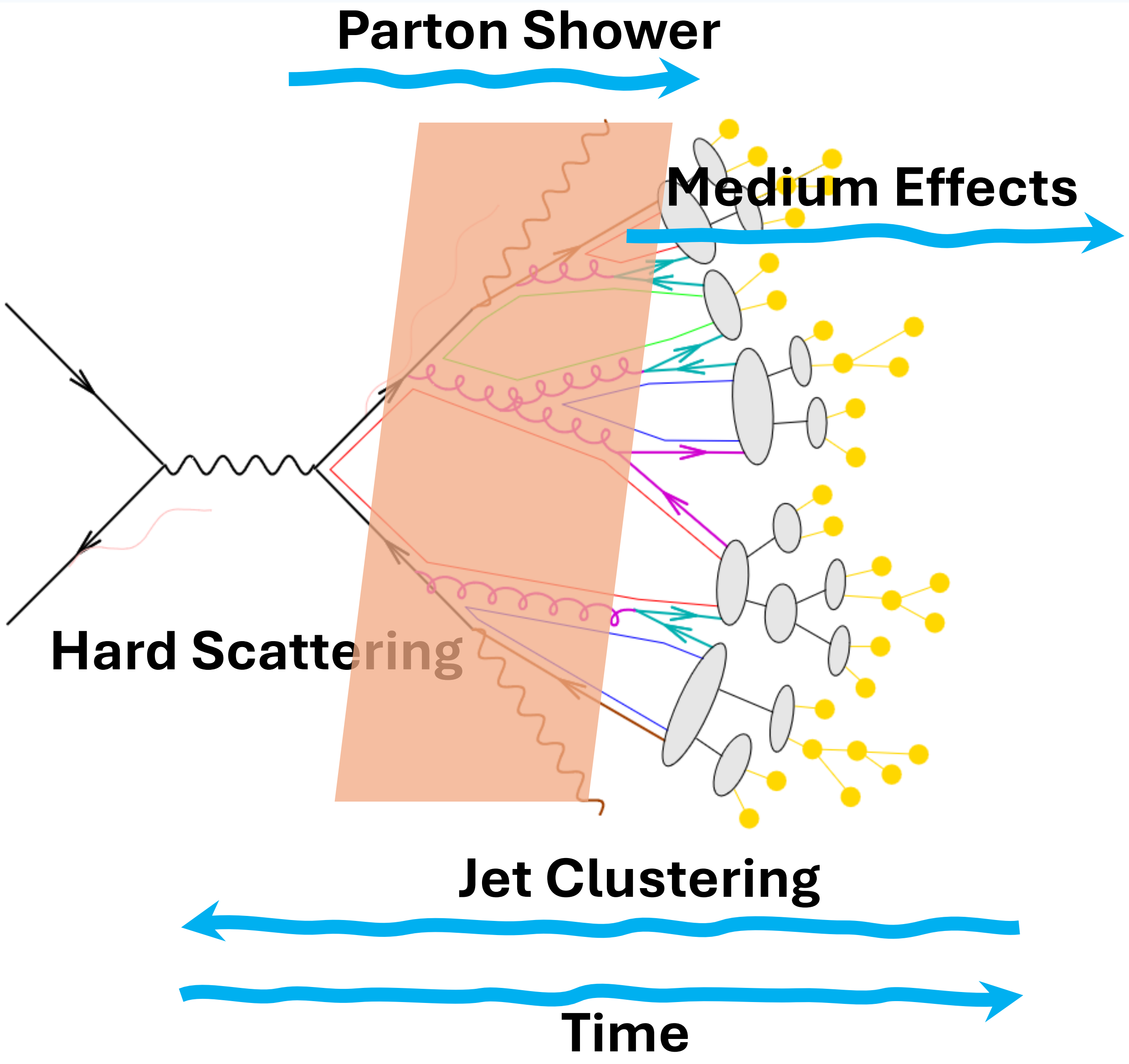
Parton Shower
Medium Effects
Hard Scattering
Jet Clustering
Time

# Jets in HIC

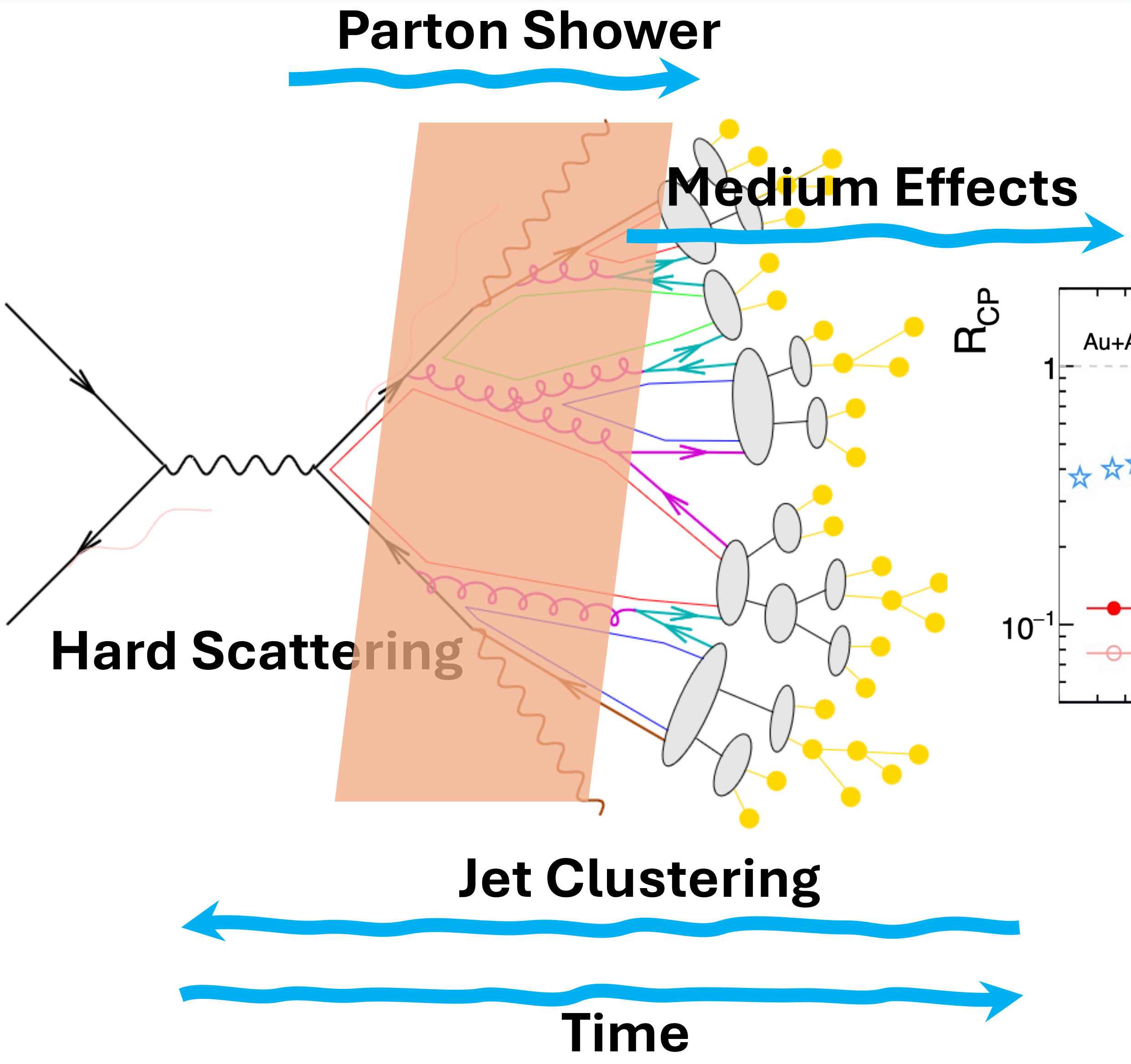


***ALICE**, JHEP03 (2014) 013*
***STAR**, Phys.Rev.C 102 (2020) 5, 054913*

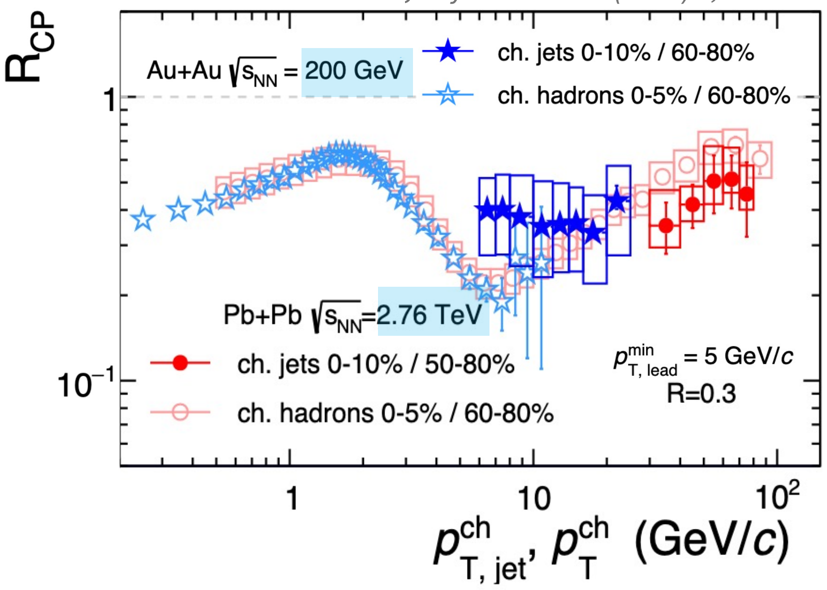


Energy Loss

***CMS**, Phys. Lett. B 730 (2014) 243*

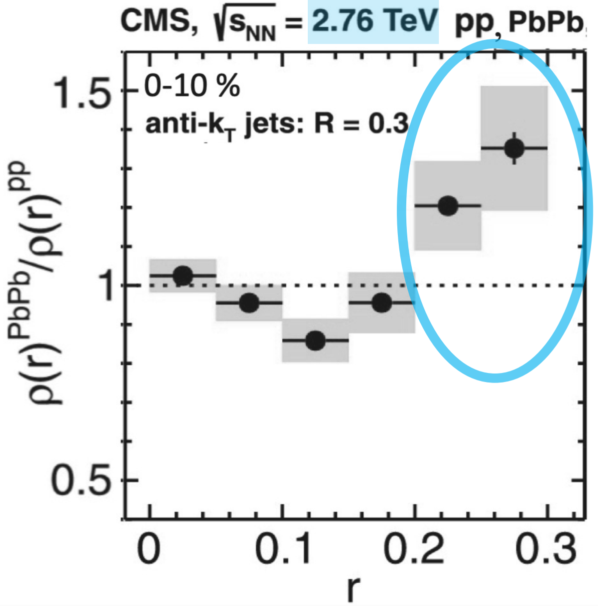


Jet Broadening

# Jets in HIC: Substructure Modifications

**Generalized Angularities**

$$\lambda_\beta^\kappa = \sum_{\text{const}\in\text{jet}} \overbrace{\left(\frac{p_{\text{T,const}}}{p_{\text{T,jet}}}\right)^\kappa}^{\text{soft/hard radiation}} \times \overbrace{r(\text{const},\text{jet})^\beta}^{\text{collinearity sensitive}}$$

$\lambda_1^1 = g$ - girth

$\lambda_2^1$ - thrust

$\lambda_0^2 = (p_T^D)^2$ - momentum dispersion

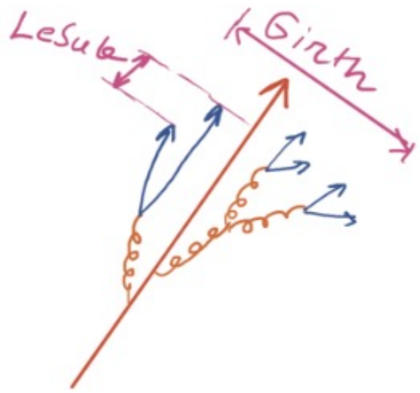


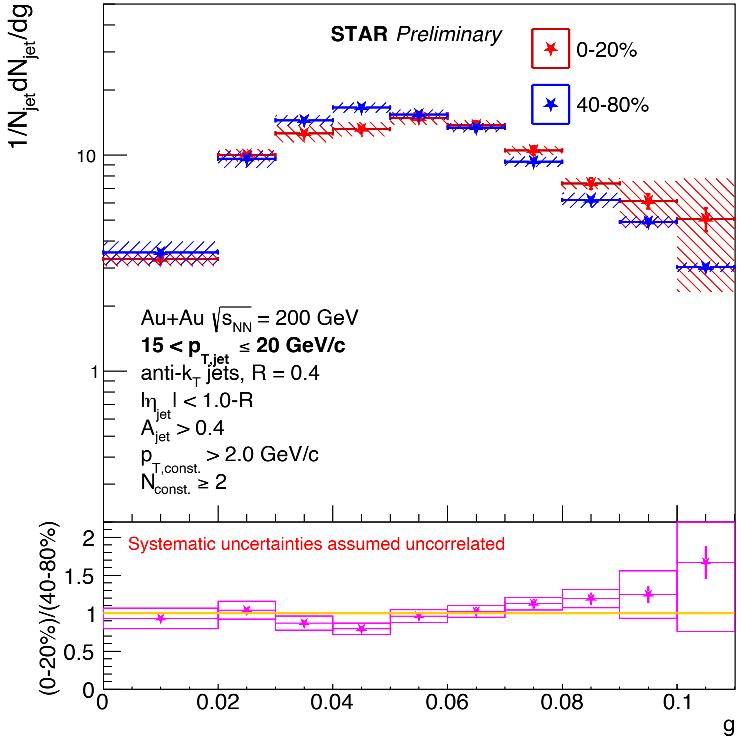


- Angularities, tunable sensitivity to energy and angular scales of jet evolution
- Can probe the modification of radiation pattern in medium

*Poster #97: Tanmay Pani*

**Ongoing measurement at STAR to quantify substructure modifications**

# Medium Effects

Elastic
collisions
(collisional)

Medium Wake

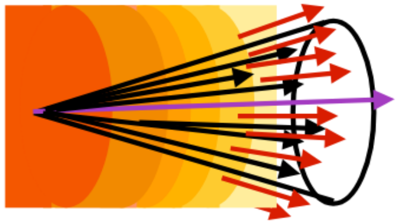

Inelastic
collisions
(radiative)

Medium-induced Splitting

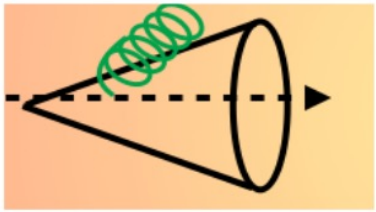

Cartoons courtesy Laura Havener (Yale)

Medium response depends on mass and flavor of the underlying parton

**Motivation to study**

**heavy flavor tagged jets**

# HF Jets In Vacuum

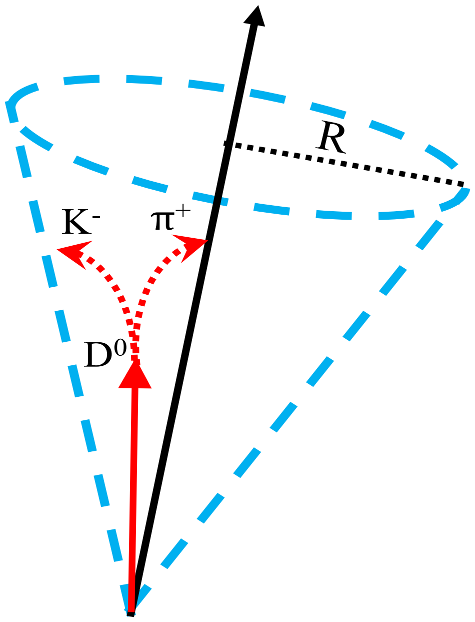


## Radiation Pattern of Charm in Vacuum

$$R(\theta) = \frac{1}{N^{D^0\,\text{jets}}} \frac{dn^{D^0\,\text{jets}}}{d\ln(1/\theta)} \Big/ \frac{1}{N^{\text{inclusive jets}}} \frac{dn^{\text{inclusive jets}}}{d\ln(1/\theta)} \Bigg|_{k_T, E_{\text{Radiator}}}$$

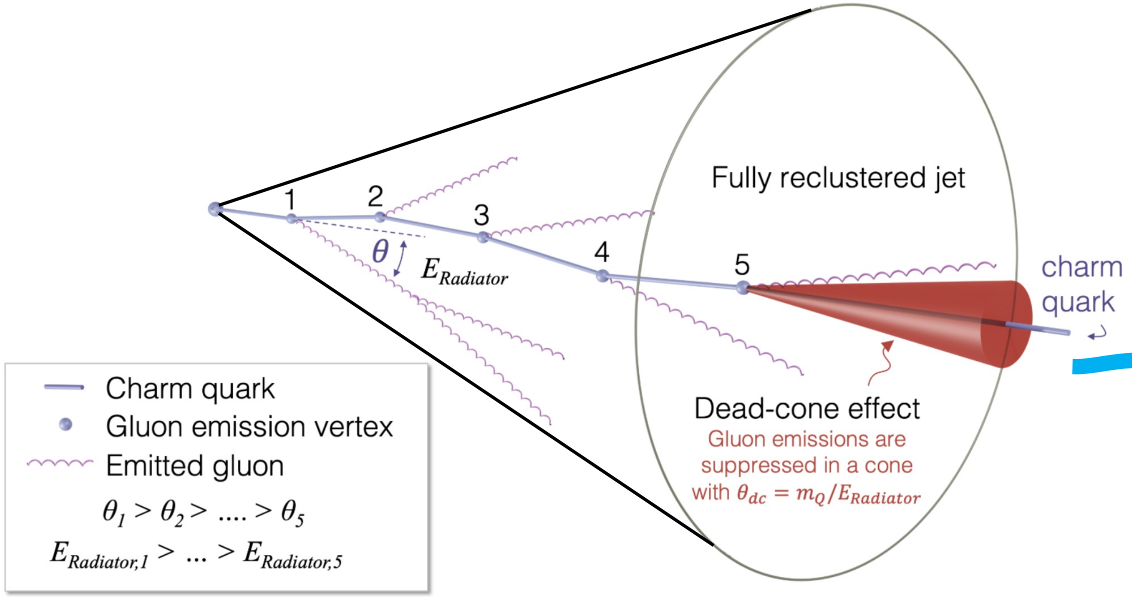


Nature volume 605, 440–446 (2022)

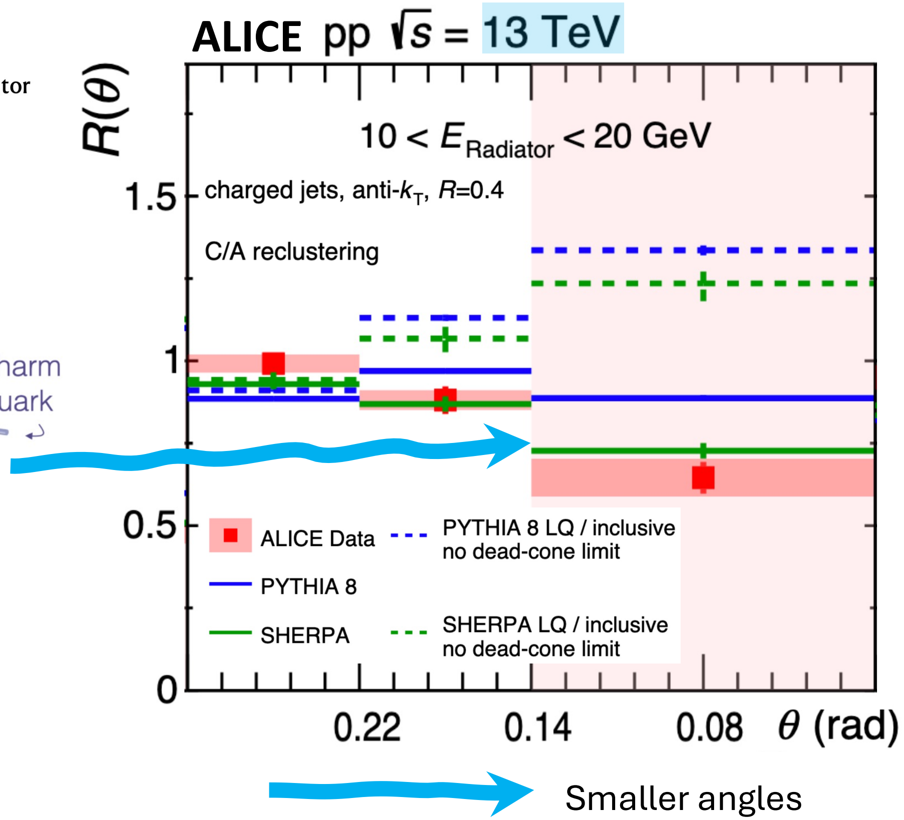


**Heavy-flavor emission spectra at small angles suppressed due to dead-cone effect**

# HF Jets In Vacuum: Fragmentation

D$^0$ Momentum Fraction → Handle on the Fragmentation Pattern for Charm

$$z_{//}^{ch} = \frac{\vec{p}_{\text{ch jet}} \cdot \vec{p}_{\text{HF}}}{\vec{p}_{\text{ch jet}} \cdot \vec{p}_{\text{ch jet}}}$$

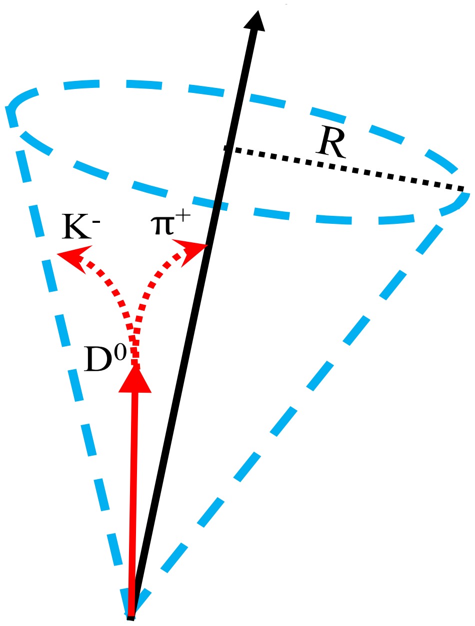

# HF Jets In Vacuum: Fragmentation

$D^0$ Momentum Fraction → Handle on the Fragmentation Pattern for Charm

$$z_{//}^{ch} = \frac{\vec{p}_{ch\ jet} \cdot \vec{p}_{HF}}{\vec{p}_{ch\ jet} \cdot \vec{p}_{ch\ jet}}$$

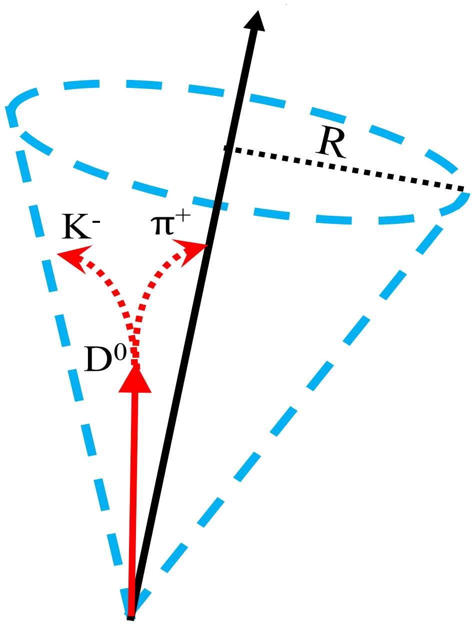


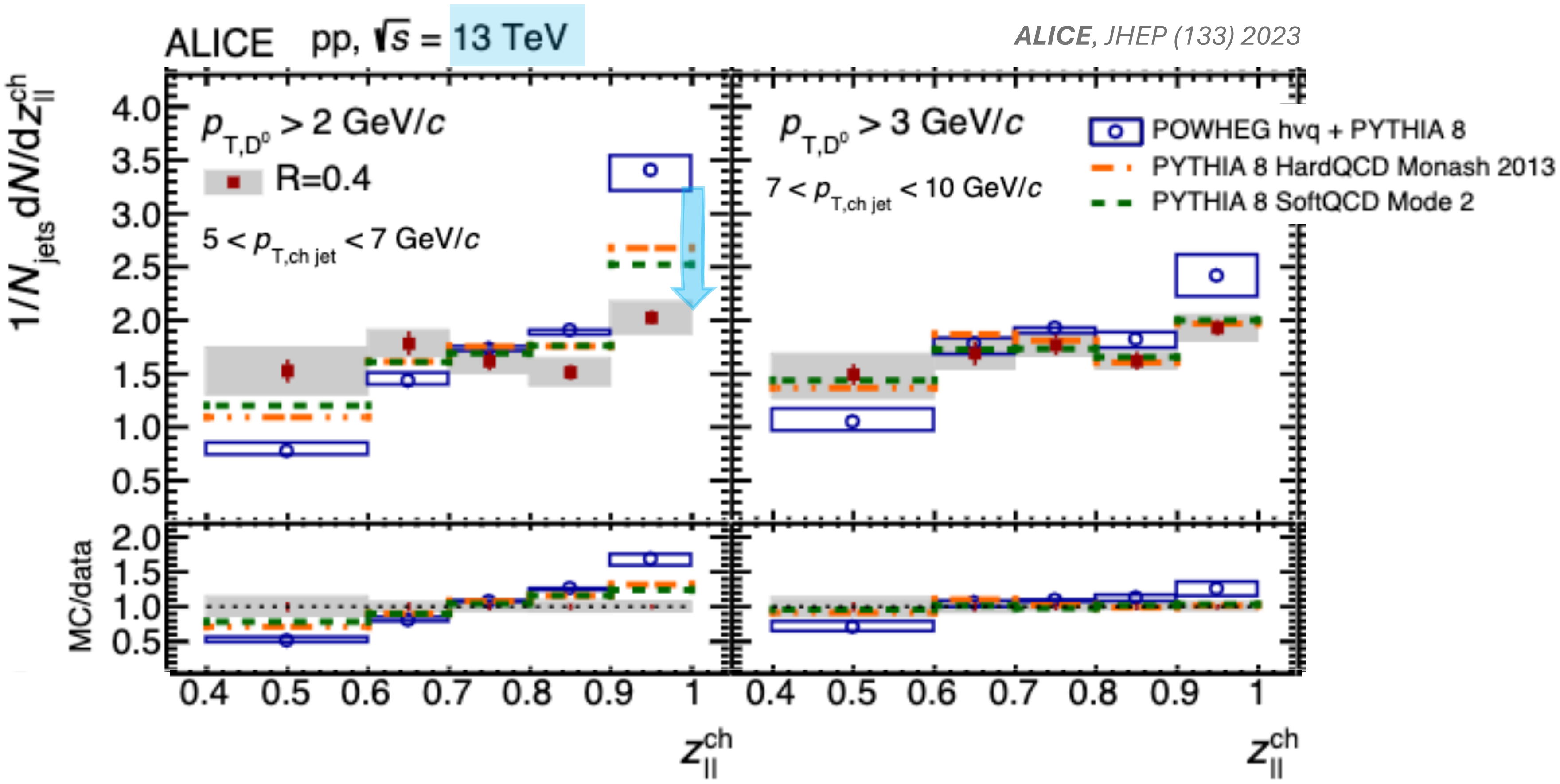

# HF Jets In Vacuum: Fragmentation

$D^0$ Momentum Fraction → Handle on the Fragmentation Pattern for Charm

$$z_{//}^{ch} = \frac{\vec{p}_{ch\,jet} \cdot \vec{p}_{HF}}{\vec{p}_{ch\,jet} \cdot \vec{p}_{ch\,jet}}$$

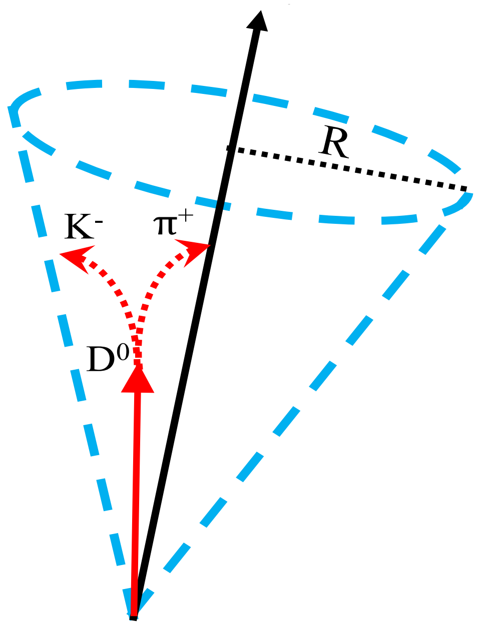


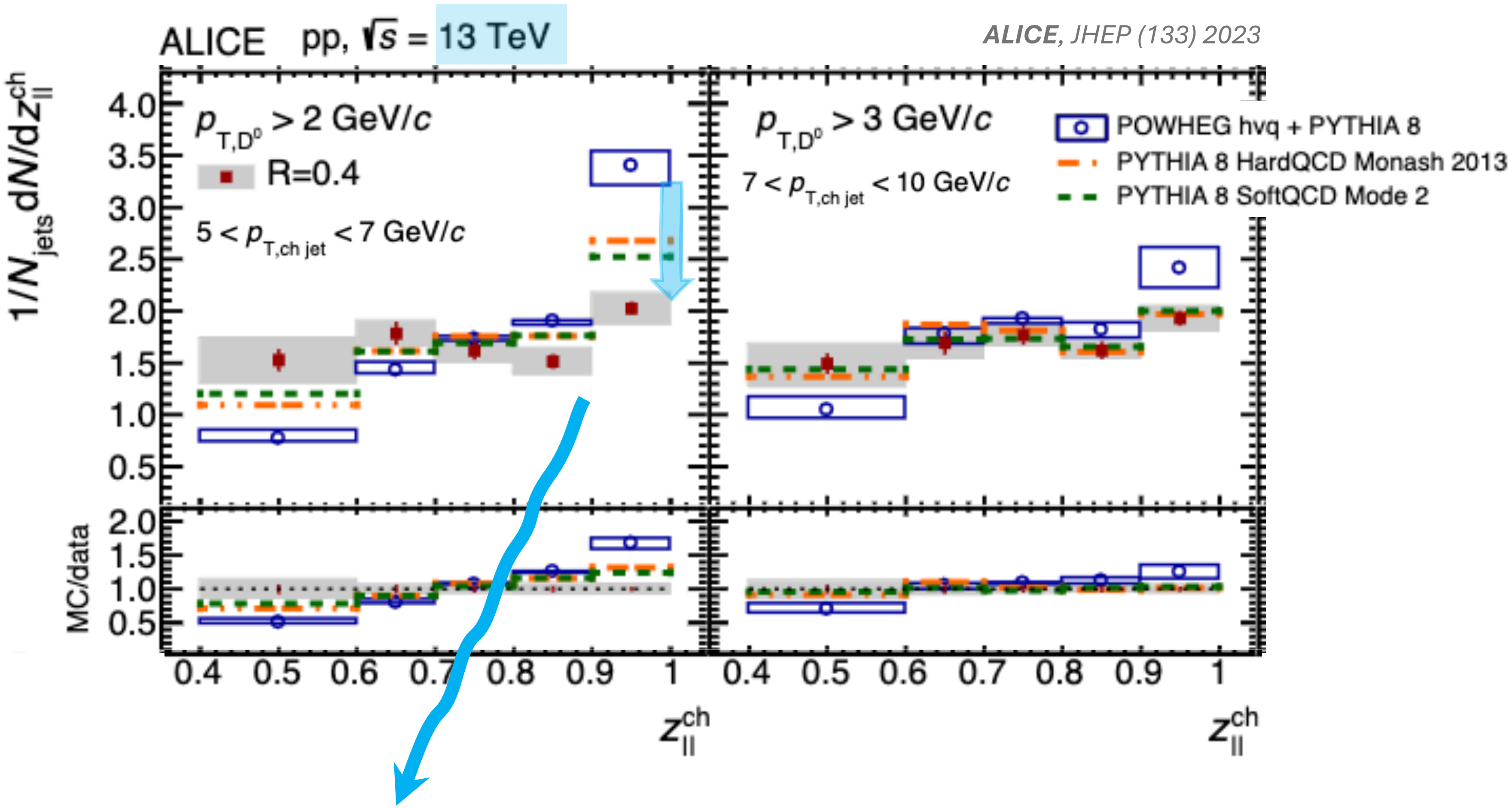


**Softer fragmentation for low energy jets compared to models**

# HF Jets In HIC: Radial Profile

Radial Profile of $D^0$ → Access to in-medium diffusion

***CMS,*** *Phys. Rev. Lett. 125 (2020) 102001*

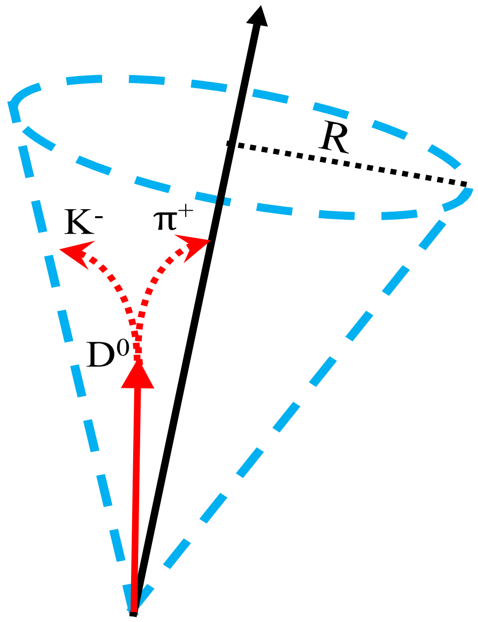


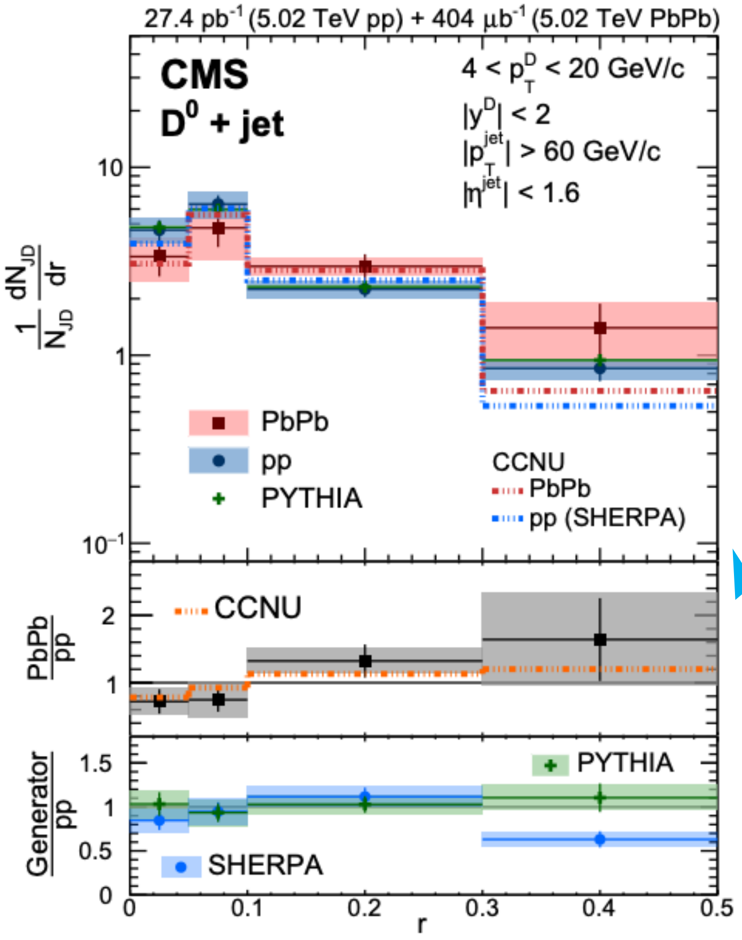


**Hint of diffusion for low $p_T$ $D^0$ mesons in the presence of QGP at LHC**

# HF Jets In HIC: Radial Profile

Radial Profile of $D^0$ → Access to in-medium diffusion

***CMS,** Phys. Rev. Lett. 125 (2020) 102001*

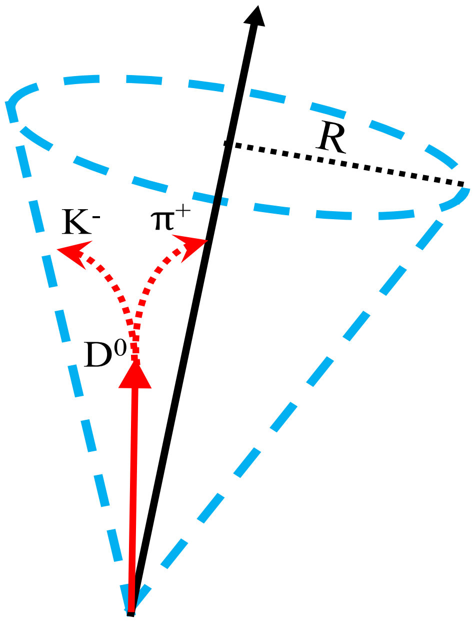


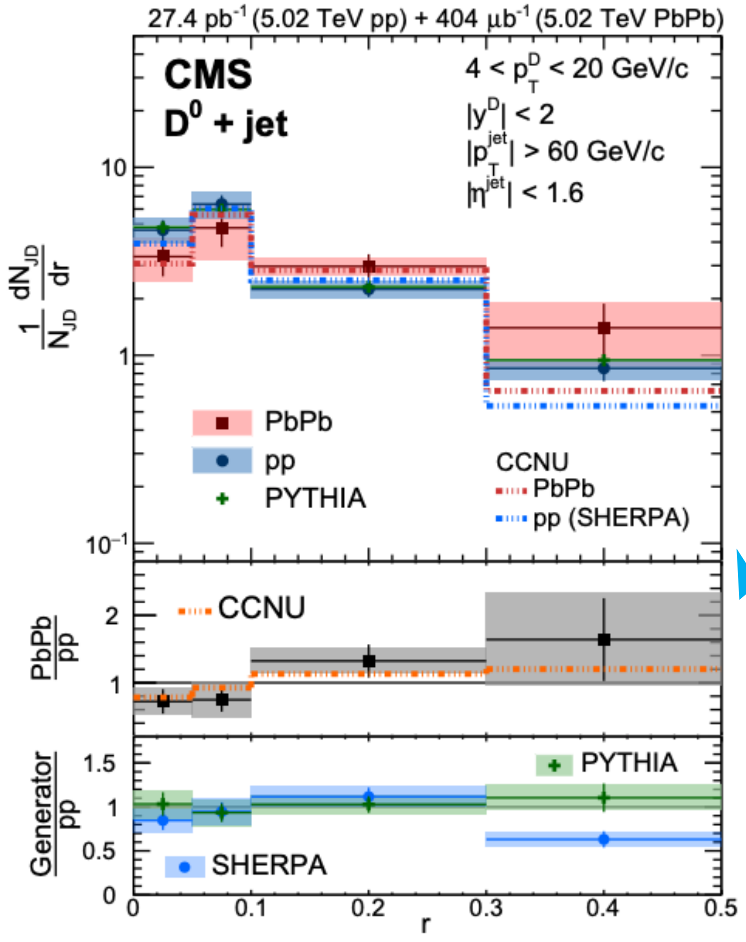


**Hint of diffusion for low $p_T$ $D^0$ mesons in the presence of QGP at LHC**

- Lower $p_T$ $D^0$ mesons accessible at STAR
- Contribution from the underlying background smaller for Au + Au $\sqrt{s_{NN}}$ = 200 GeV

# The Detector

# STAR at RHIC

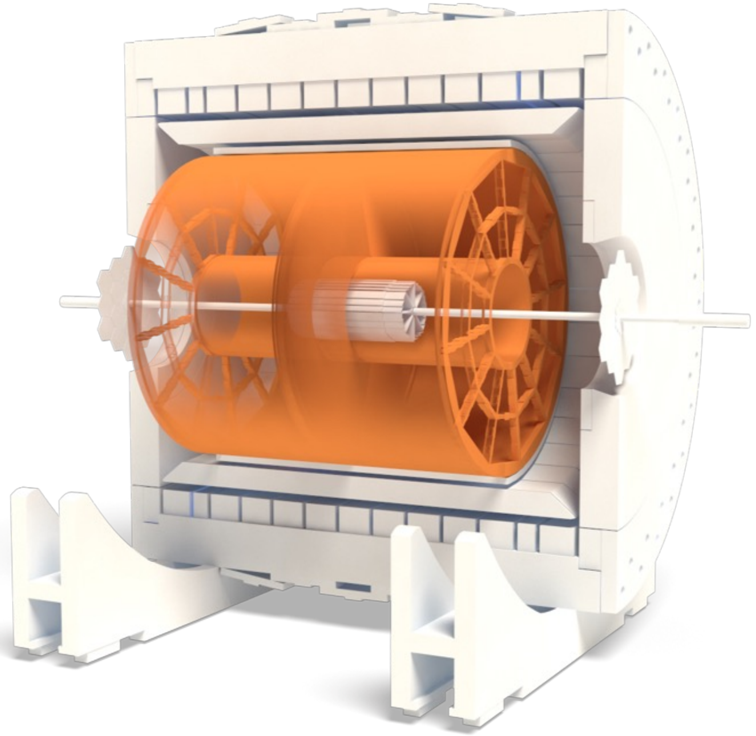

**Time Projection Chamber**

- ✓ Measures momenta of charged tracks $[|\eta| < 1, 0 < \phi < 2\pi]$
- ✓ PID using dE/dx

*Images: NSWW*

# STAR at RHIC

**Time-Of-Flight Detector**

- ✓ PID using TOF measurement $[|\eta| < 1, 0 < \phi < 2\pi]$

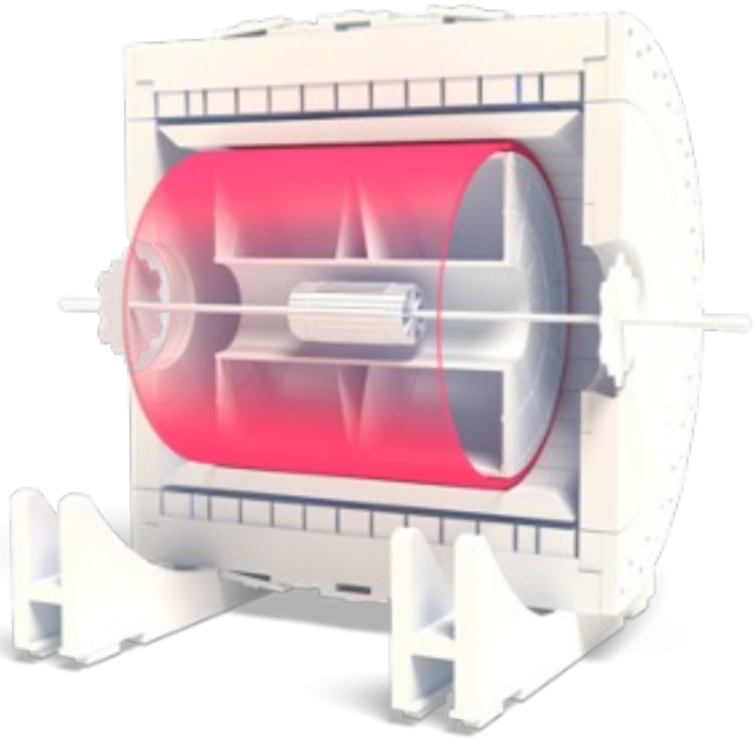

**Time Projection Chamber**

- ✓ Measures momenta of charged tracks $[|\eta| < 1, 0 < \phi < 2\pi]$
- ✓ PID using dE/dx

*Images: NSWW*

# STAR at RHIC

**Time-Of-Flight Detector**

- ✓ PID using TOF measurement $[|\eta| < 1, 0 < \phi < 2\pi]$

**Barrel Electromagnetic Calorimeter**

- ✓ Measures neutral component of jet energy $[|\eta| < 1, 0 < \phi < 2\pi]$

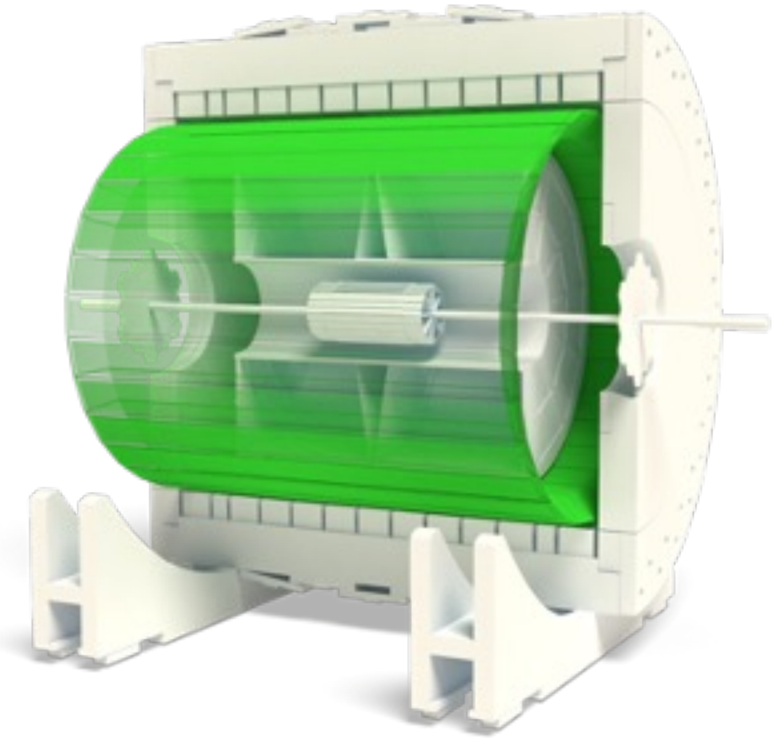

**Time Projection Chamber**

- ✓ Measures momenta of charged tracks $[|\eta| < 1, 0 < \phi < 2\pi]$
- ✓ PID using dE/dx

*Images: NSWW*

# STAR at RHIC

**Time-Of-Flight Detector**

- ✓ PID using TOF measurement $[|\eta| < 1, 0 < \phi < 2\pi]$

**Barrel Electromagnetic Calorimeter**

- ✓ Measures neutral component of jet energy $[|\eta| < 1, 0 < \phi < 2\pi]$

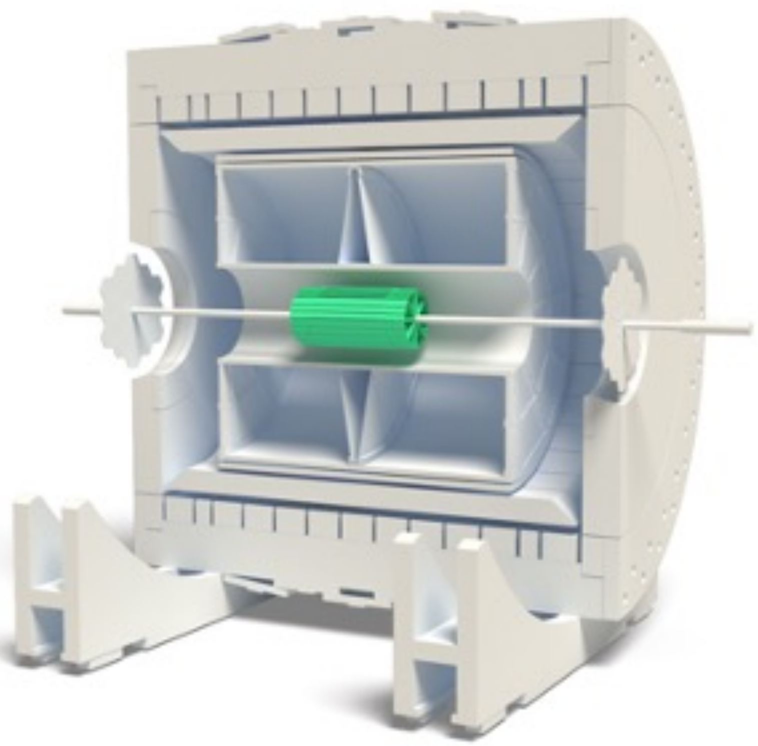

**Time Projection Chamber**

- ✓ Measures momenta of charged tracks $[|\eta| < 1, 0 < \phi < 2\pi]$
- ✓ PID using dE/dx

**Heavy Flavor Tracker** (2014-2016)

- ✓ Improves position resolution for secondary vertices

*Images: NSWW*

# Methods

# Analysis Details

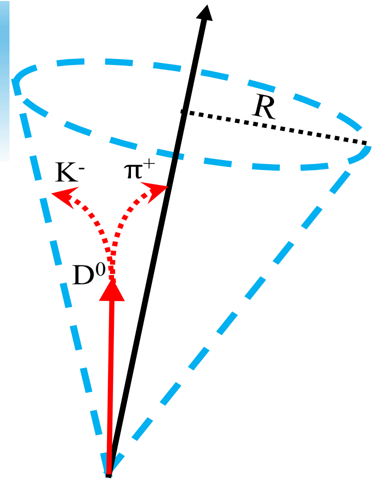


- **Au + Au 200 GeV Run 2014, ~1B events**
- **Centrality ∈ [0, 80]% (3 bins: [0-10]%, [10-40]%, [40-80]%)**
- $0.2 < p_{\mathrm{T,track}}$ [GeV/*c*] < 30 ; $0.2 < E_{\mathrm{T,tower}}$ [GeV] < 30
- $|\eta_{\mathrm{track}}| < 1$ ; $|\eta_{\mathrm{tower}}| < 1$
- $D^0 \rightarrow K^{\mp} + \pi^{\pm}$ [B.R. = 3.82 %]
- For $D^0$ reconstruction: Tracks contain at least three hits on HFT
- $1 < p_{\mathrm{T},D^0}$ [GeV/*c*] < 10
- **$K^{\mp}, \pi^{\pm}$ originating from $D^0$ replaced with $D^0$ in the event record before jet clustering**
- Anti-$k_{\mathrm{T}}$ full jets of radius $R$ = 0.2, 0.3, 0.4, area-based background subtraction
- $|\eta_{\mathrm{Jet}}| < 1 - \mathrm{R}$
- 2D unfolding done for [Jet $p_{\mathrm{T}}$, $D^0$ transverse momentum fraction] and [Jet $p_{\mathrm{T}}$, radial profile]

# $D^0$ Reconstruction at STAR

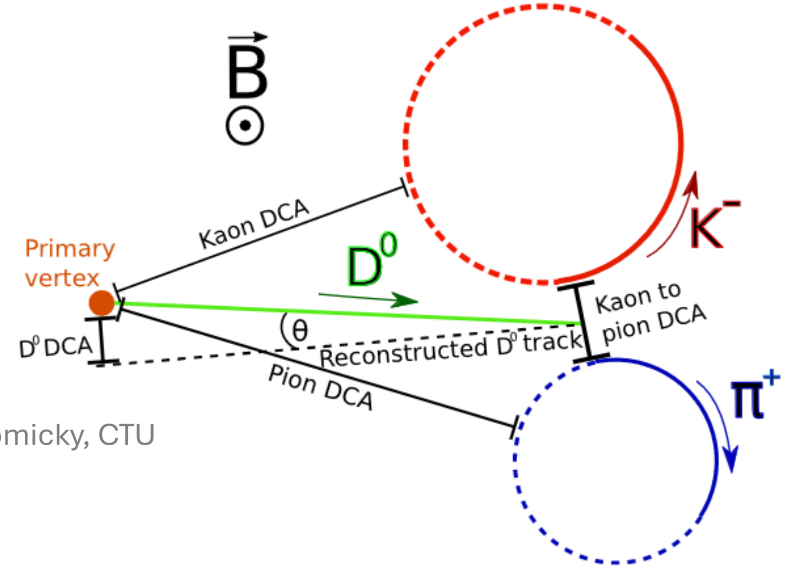


Cartoon courtesy Ondrej Lomicky, CTU

- Topological cuts to improve signal significance of $D^0$

# $D^0$ Reconstruction at STAR

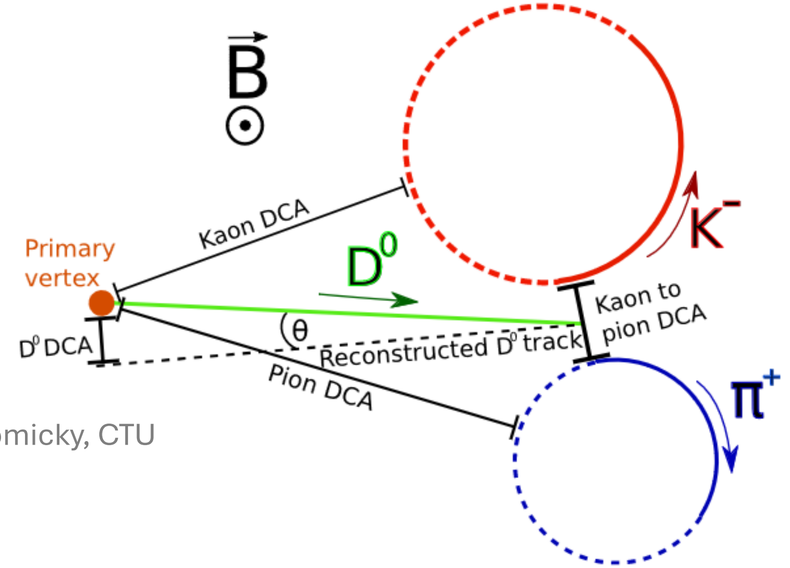


Cartoon courtesy Ondrej Lomicky, CTU

- Topological cuts to improve signal significance of $D^0$
- Yield calculation using sPlot method

*Nucl. Instrum. Methods Phys. Res., A (2005) 555*

$_s\mathcal{P}lot$

$$_s\mathcal{P}_n(m_{K\pi,i}) = \frac{\sum_{j=1}^{N_T} V_{nj} f_j(m_{K\pi,i})}{\sum_{k=1}^{N_T} N_k f_k(m_{K\pi,i})}$$

***n*** = $n^{th}$ fit component(sig/bkg)

$\boldsymbol{N_k}$ = $k^{th}$ yield (**T=2**)

$\boldsymbol{f_k(m_{K\pi,i})}$ = per-event PDF value with $k^{th}$ hypothesis

**V** = cov. matrix

Efficiency Correction

$$_s\mathcal{P}_n(m_{K\pi,i}) \rightarrow \frac{_s\mathcal{P}_n(m_{K\pi,i})}{\varepsilon(m_{K\pi,i})}$$

# $D^0$ Reconstruction at STAR

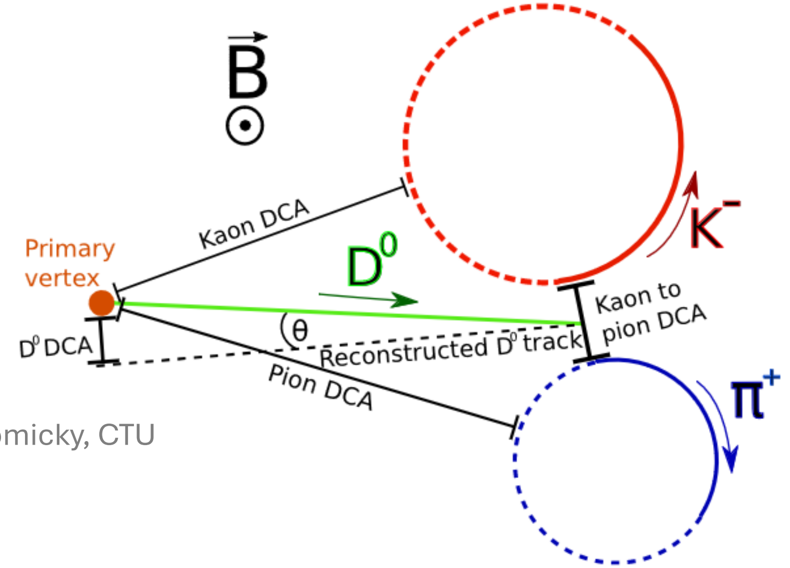


Cartoon courtesy Ondrej Lomicky, CTU

- Topological cuts to improve signal significance of $D^0$
- Yield calculation using sPlot method

*Nucl. Instrum. Methods Phys. Res., A (2005) 555*

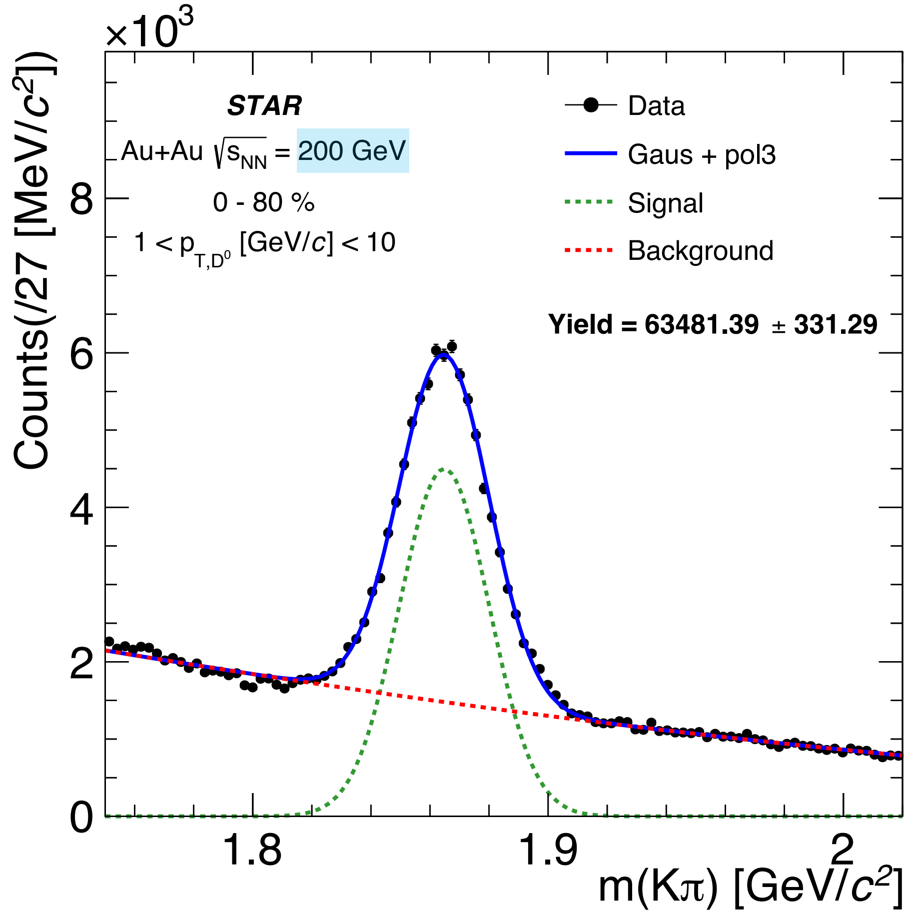


$$_s\mathcal{P}lot \quad {}_s\mathcal{P}_n(m_{K\pi,i}) = \frac{\sum_{j=1}^{N_T} V_{nj} f_j(m_{K\pi,i})}{\sum_{k=1}^{N_T} N_k f_k(m_{K\pi,i})}$$

***n*** = $n^{th}$ fit component(sig/bkg)

***$N_k$*** = $k^{th}$ yield **(T=2)**

***$f_k(m_{K\pi,i})$*** = per-event PDF value with $k^{th}$ hypothesis

**V** = cov. matrix

Efficiency Correction

$${}_s\mathcal{P}_n(m_{K\pi,i}) \rightarrow \frac{{}_s\mathcal{P}_n(m_{K\pi,i})}{\varepsilon(m_{K\pi,i})}$$

# Corrections to Spectra

*Example prior variation*

Data-driven prior

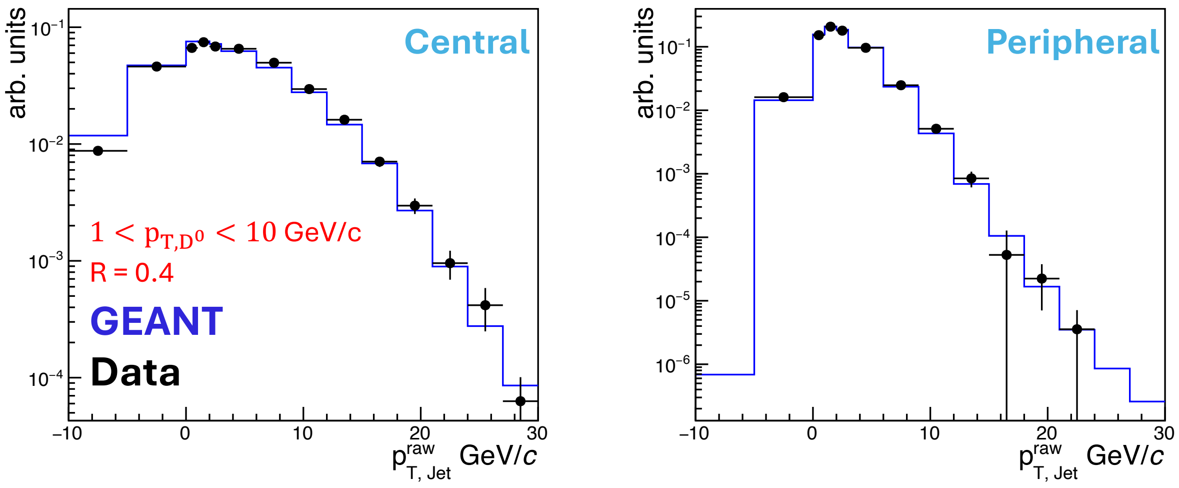


**Detector Level Jet $p_T$ [GeV/c]**

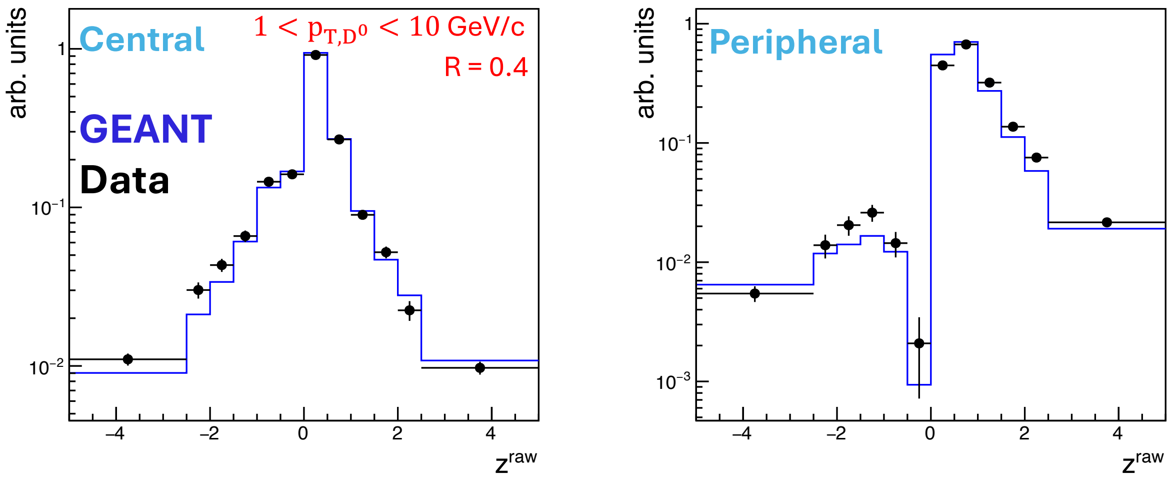


**Detector Level $D^0$ z**

**In the absence of a well-agreed upon prior distribution, best way to vary prior input to unfolding**

**Resolve differences between detector level observables from simulation and data**

# Results

# HF Jets Yield vs $p_{T,Jet}$

Function of Jet Transverse Momentum and Centrality

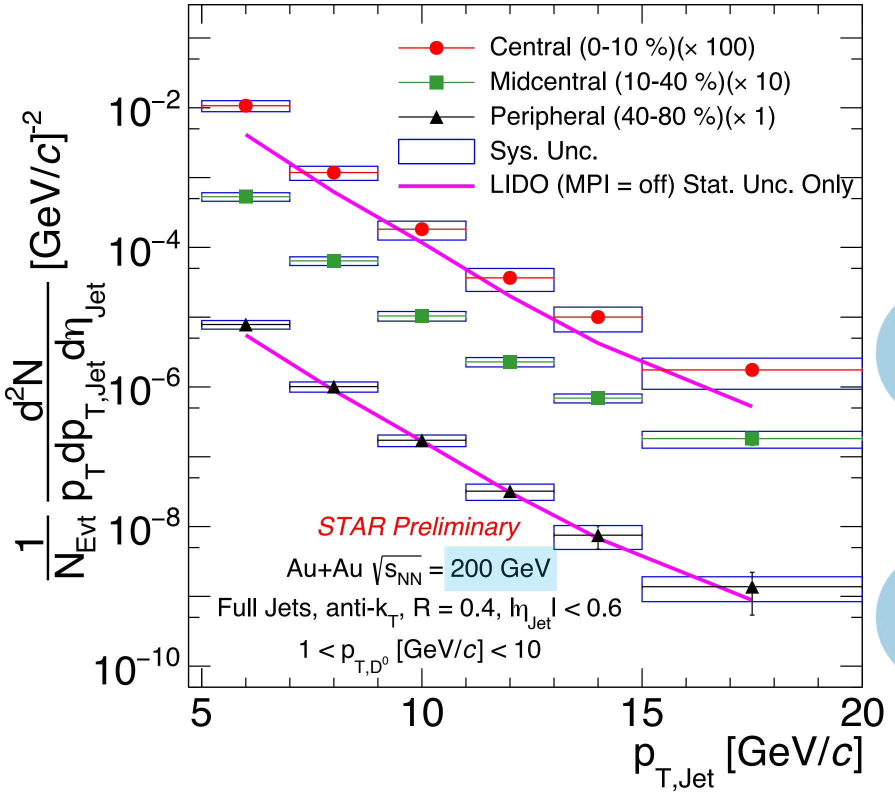


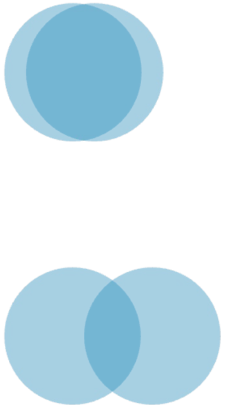

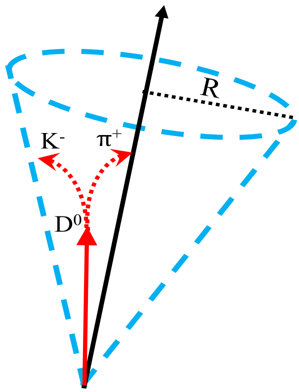


*LIDO, Phys. Rev. C 98, 064901*

# HF Jets Yield vs $p_{T,Jet}$

Function of Jet Transverse Momentum and Centrality

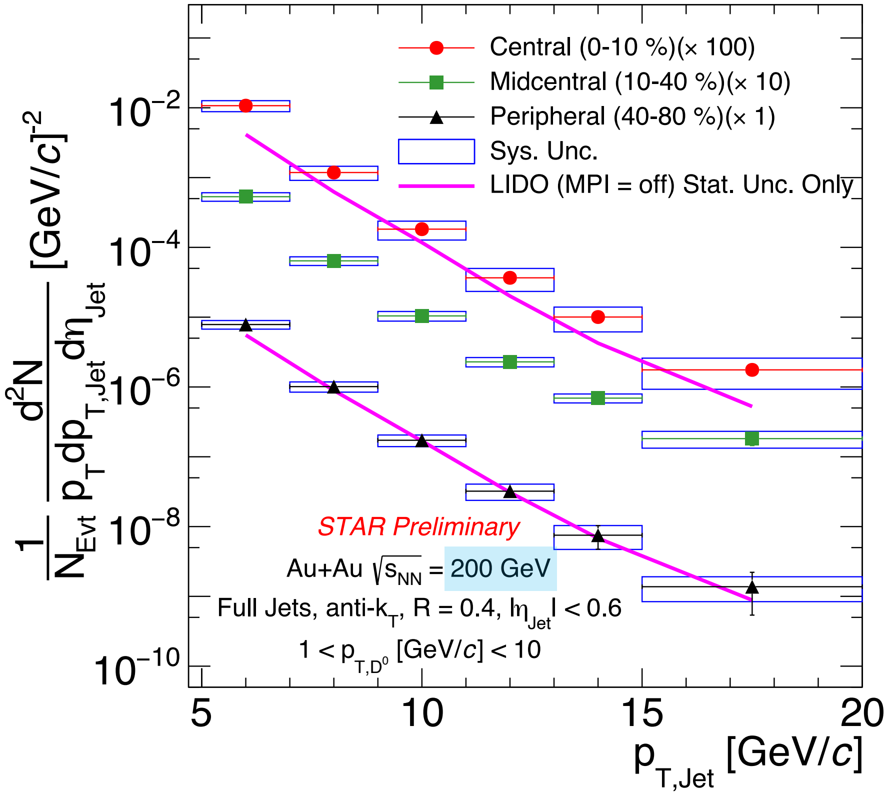


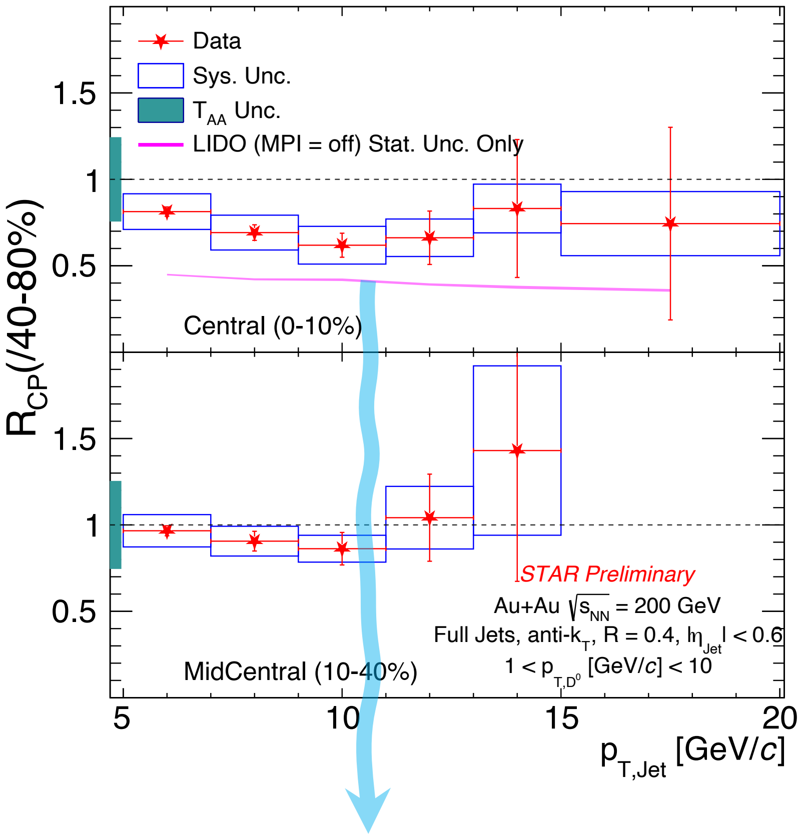


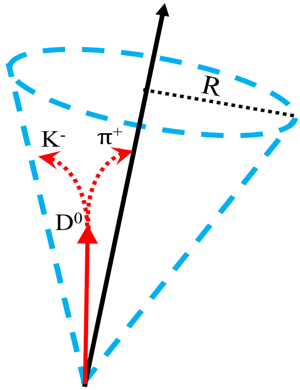


- LIDO explains peripheral yield well, slightly underpredicts yield in central events
- MPI effects important for low $p_{T,D^0}$ jet yield

*LIDO, Phys. Rev. C 98, 064901*

**Hint of suppression for $D^0$ jet yield in central collisions**

# HF Jets Yield vs z

Function of Jet Transverse Momentum Fraction and Centrality

$$z_{\text{Jet}} = \frac{\vec{p}_{\text{T,Jet}} \cdot \vec{p}_{\text{T,D}^0}}{|\vec{p}_{\text{T,Jet}}|^2}$$

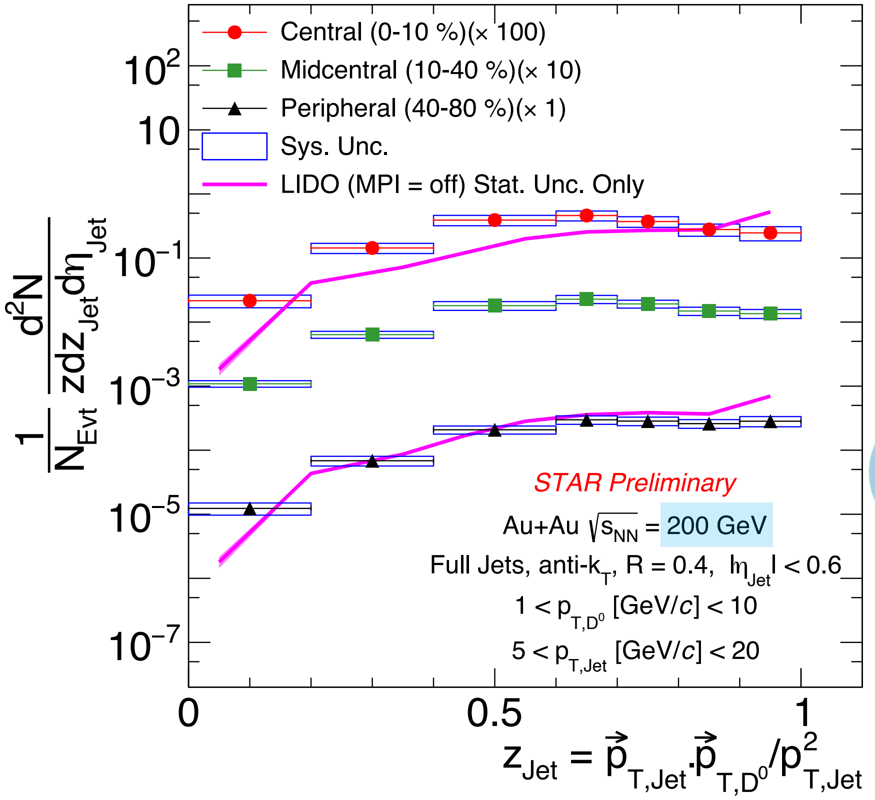


LIDO, Phys. Rev. C 98, 064901

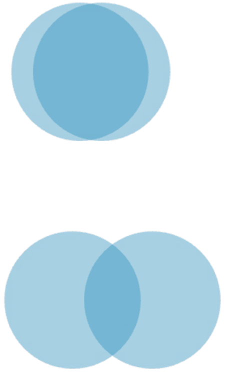

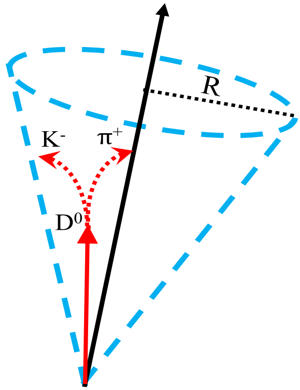

# HF Jets Yield vs z

Function of Jet Transverse Momentum Fraction and Centrality

$$z_{\text{Jet}} = \frac{\vec{p}_{\text{T,Jet}} \cdot \vec{p}_{\text{T,D}^0}}{|\vec{p}_{\text{T,Jet}}|^2}$$

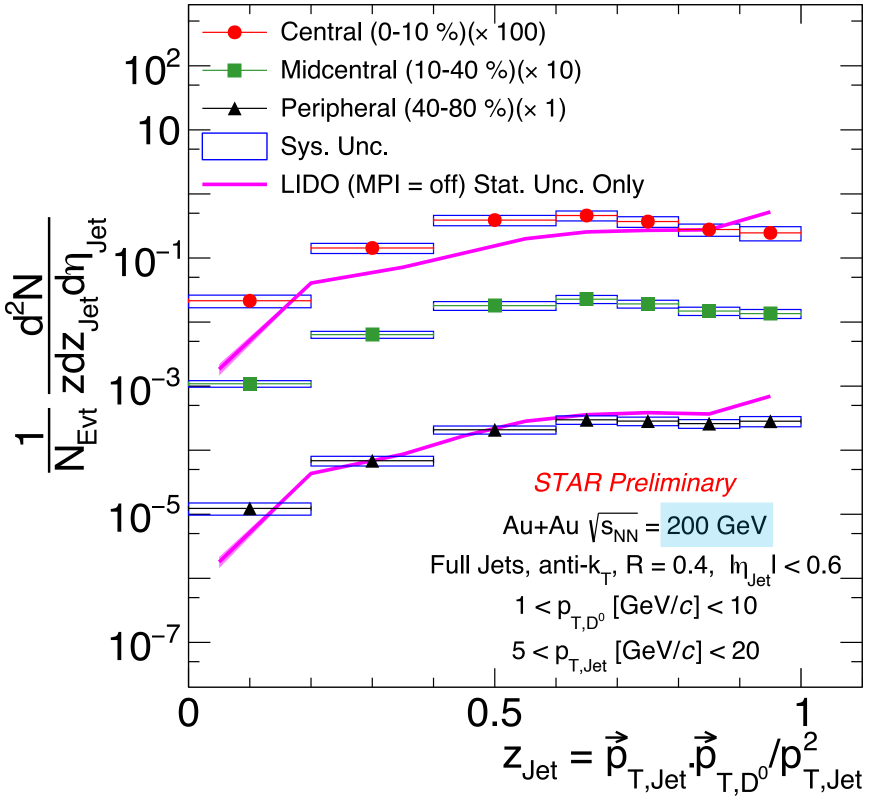


*LIDO, Phys. Rev. C 98, 064901*

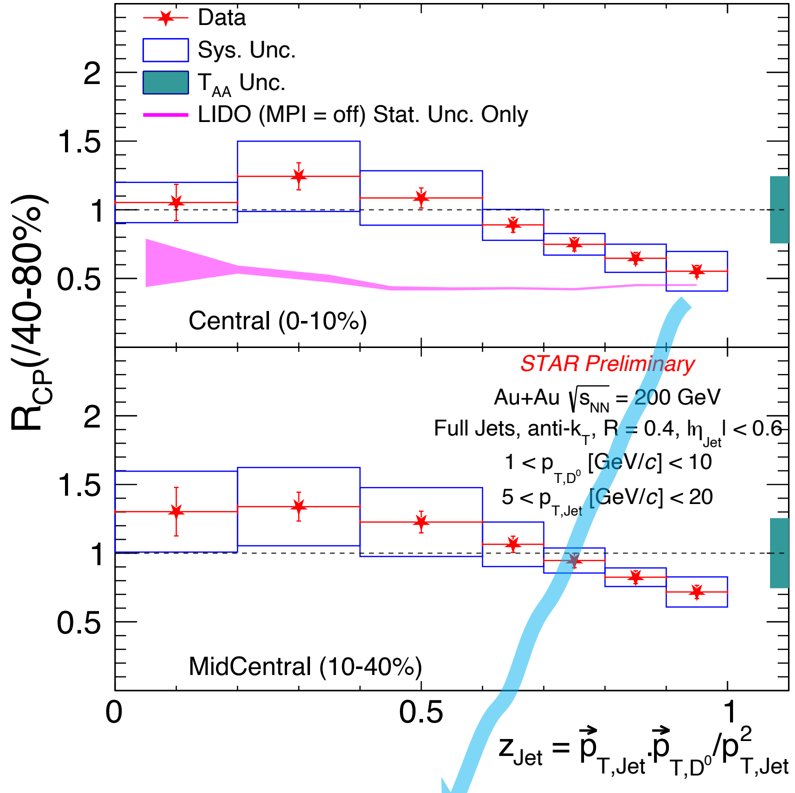


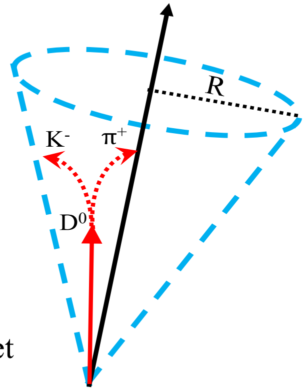


- 2D unfolded with $p_{T,Jet}$
- LIDO overestimates hard fragmented $D^0$ jets → Data shows softer fragmentation
- Soft fragmented jets yield consistent in central and peripheral collisions

**Suppression for hard fragmented $D^0$ jets in central collisions**

# HF Jets Substructure

Radial Profile of $D^0$ → Access to in-medium diffusion

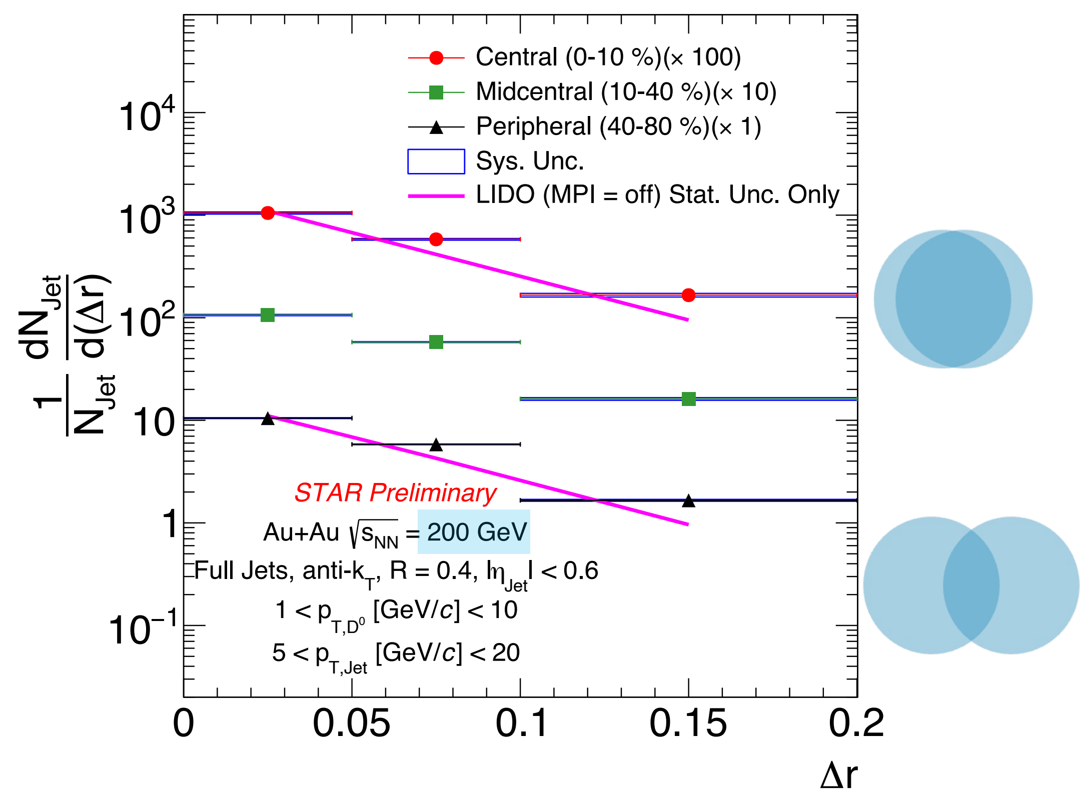


*LIDO, Phys. Rev. C 98, 064901*

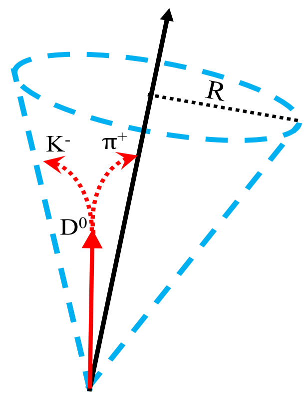

# HF Jets Substructure

Radial Profile of $D^0$ → Access to in-medium diffusion

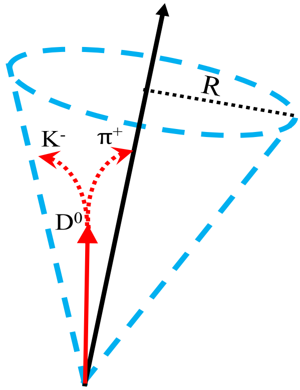


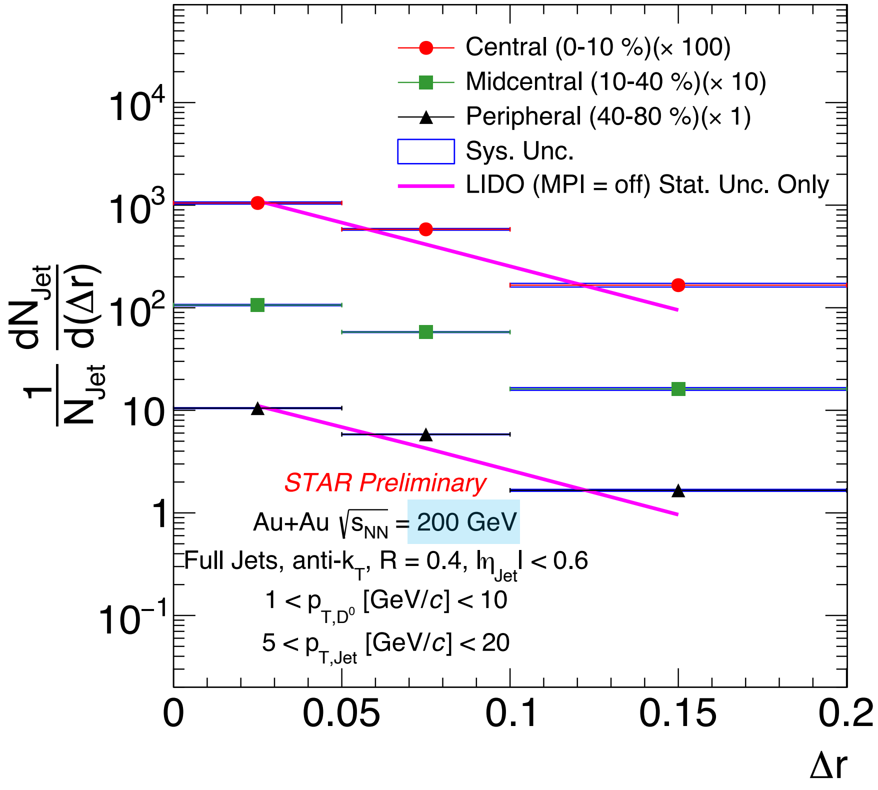


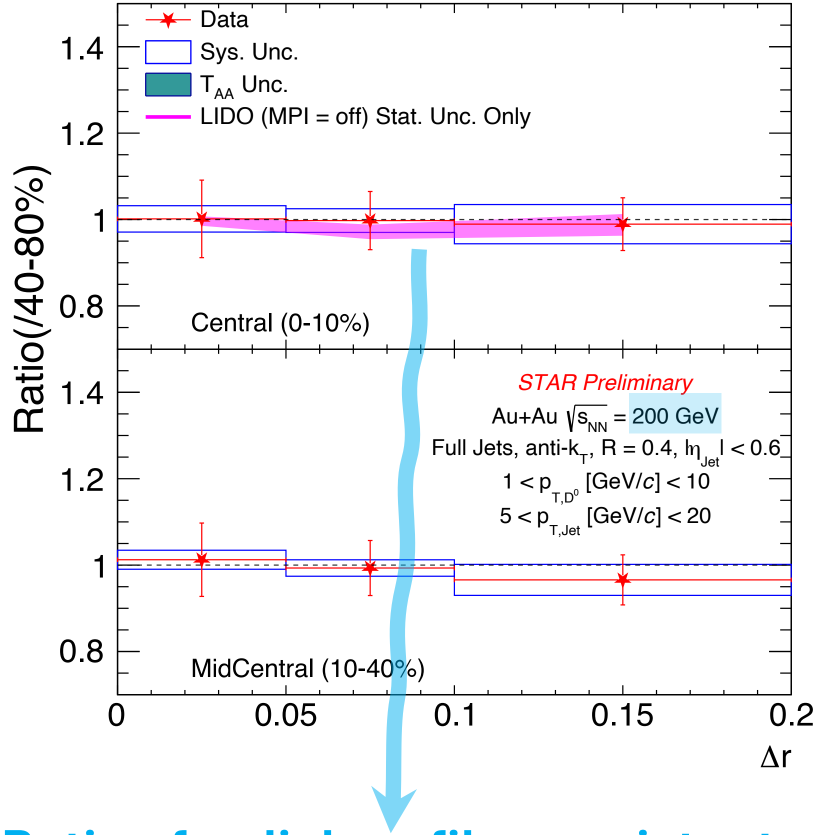


*LIDO, Phys. Rev. C 98, 064901*

**Ratio of radial profile consistent with 1**

- 2D unfolded with $p_{T,Jet}$
- LIDO qualitatively explains radial profile trends, along with ratio of central and peripheral

# HF Jets Cone Size Dependence

*LIDO, Phys. Rev. C 98, 064901*

*CCNU, Symmetry **2023**, 15(3), 727*

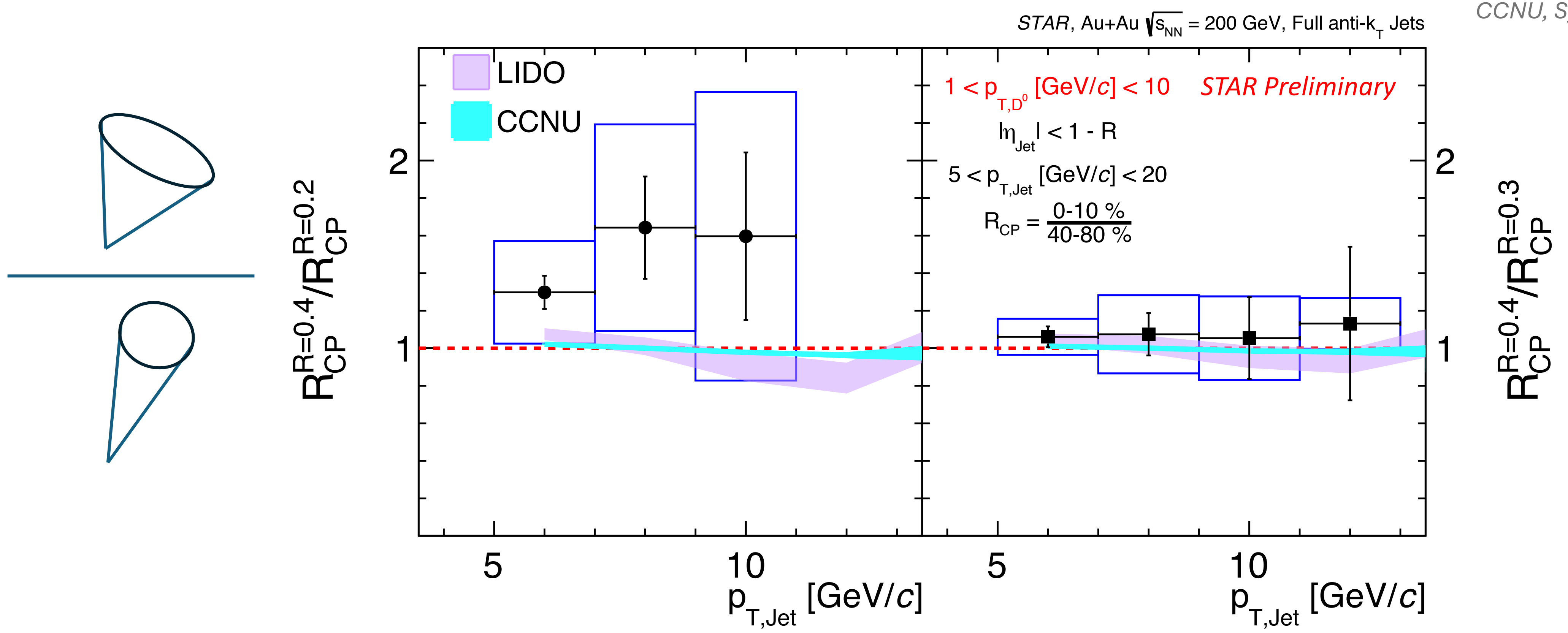


**No jet cone size dependence of medium effects observed vs $p_{T,Jet}$ within uncertainties**

# HF Jets Cone Size Dependence

*LIDO, Phys. Rev. C 98, 064901*

*CCNU, Symmetry **2023**, 15(3), 727*

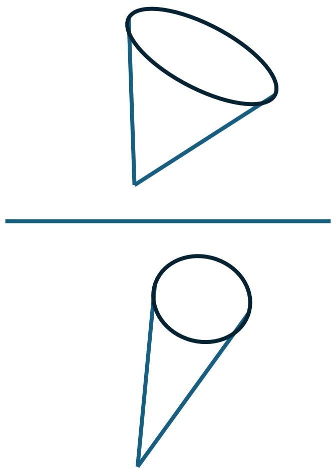

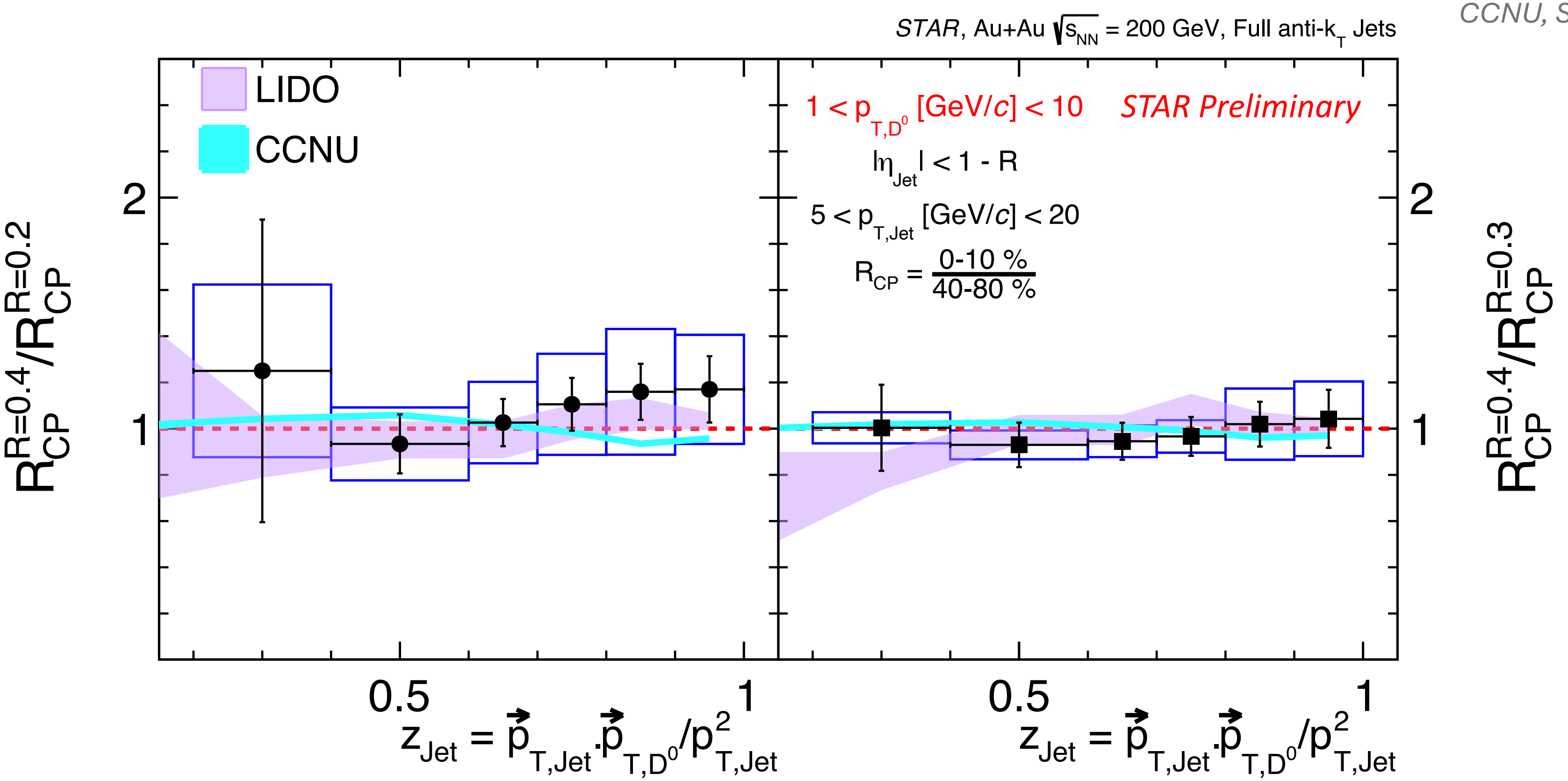


**No jet cone size dependence of medium effects observed vs z within uncertainties**

# Comparison with inclusive jets at STAR

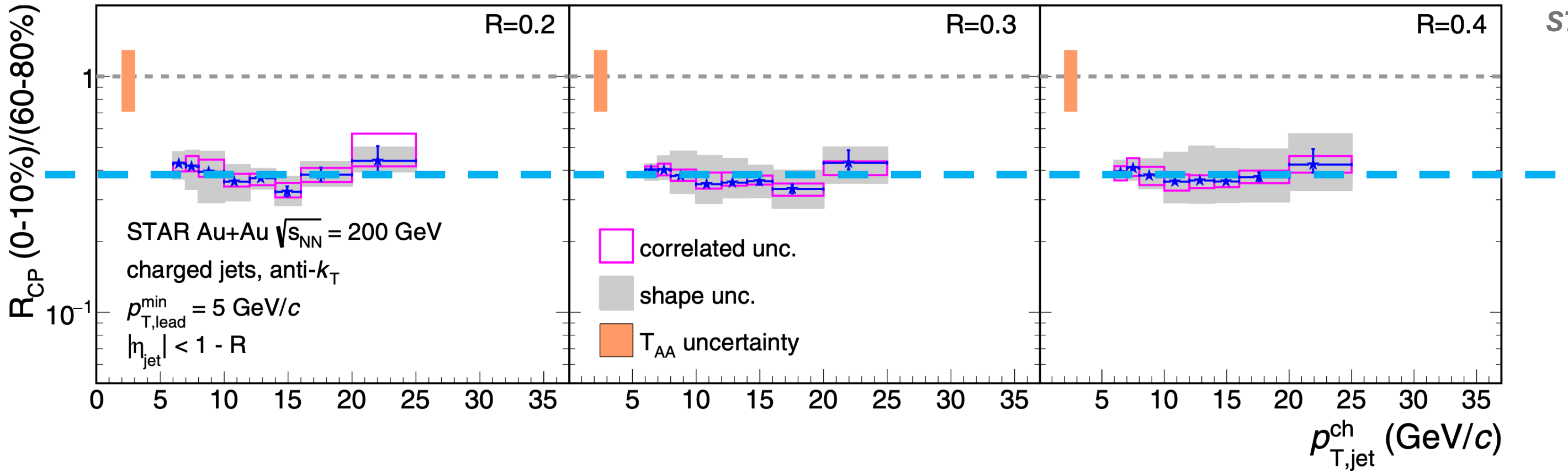


*STAR* *Phys. Rev. C* ***102****, 054913*

Similar behavior for jet cone size dependence at STAR for inclusive and $D^0$ tagged jets

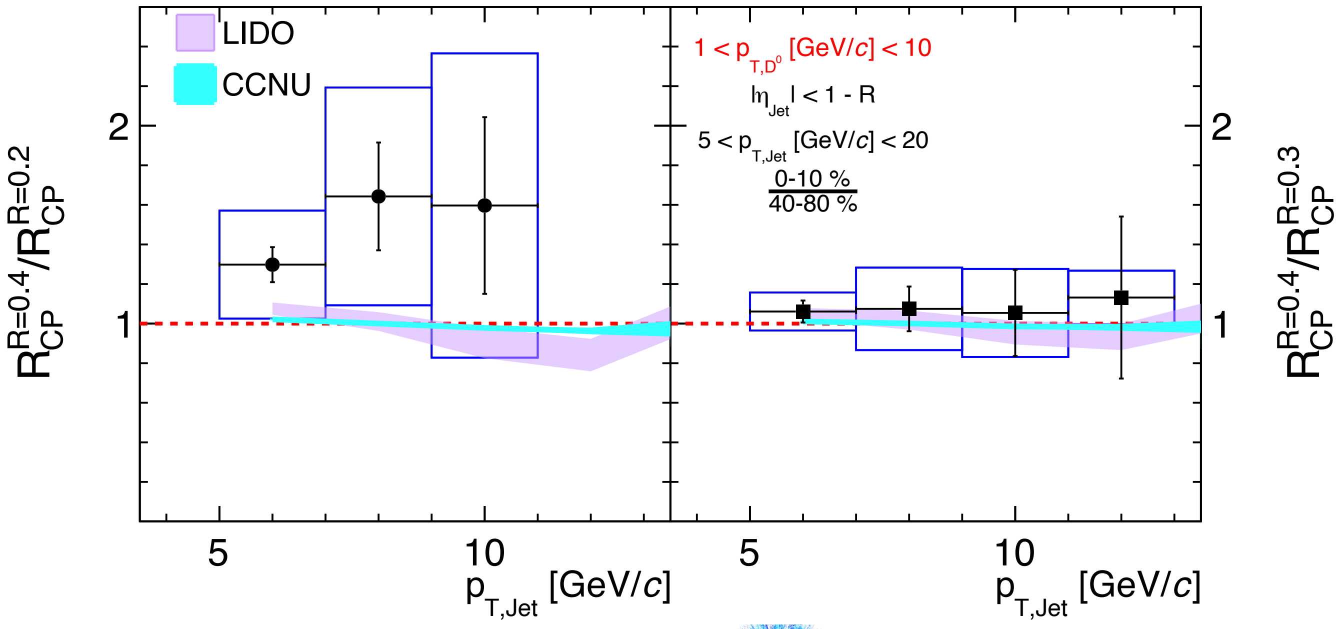

# Comparison across kinematic ranges

*STAR* *Phys. Rev. C* ***102**, 054913*

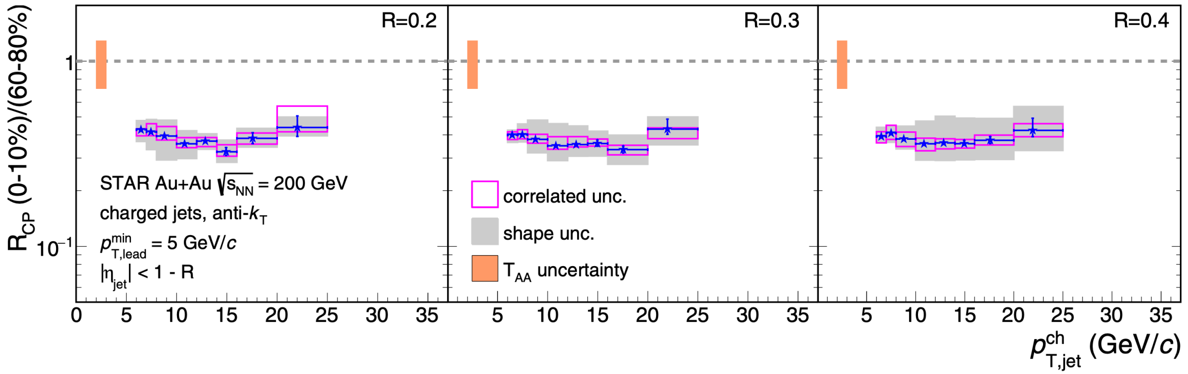


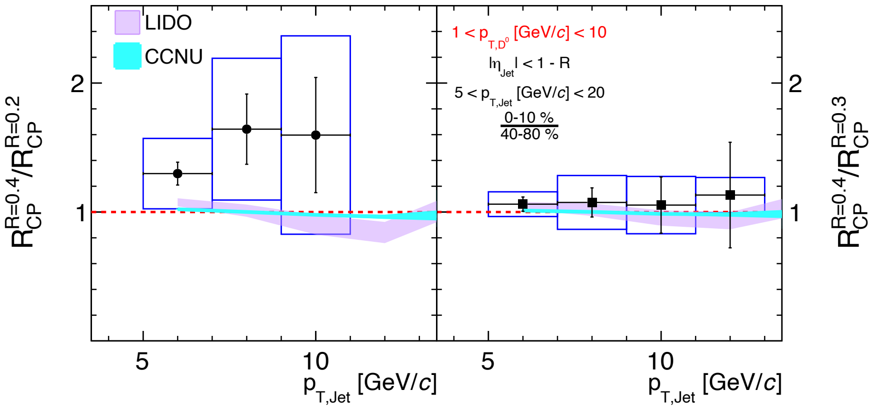


*ALICE* *Phys. Let. B* ***849**, 138412*

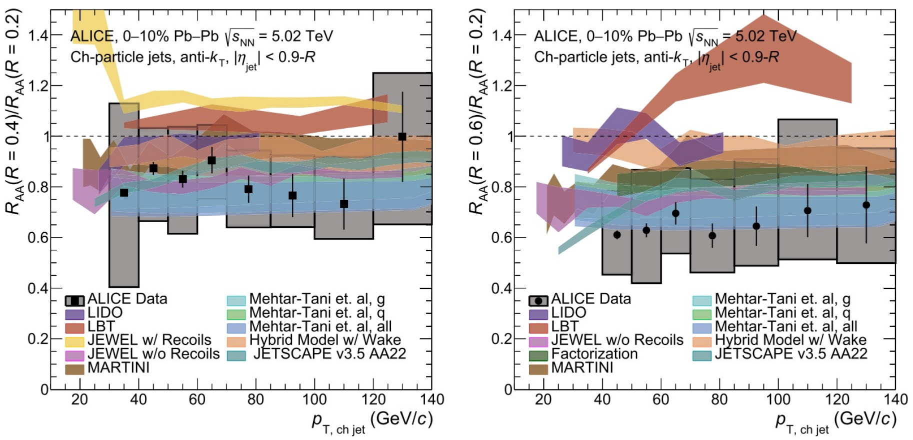


*ATLAS* *Phys. Let. B* ***719***

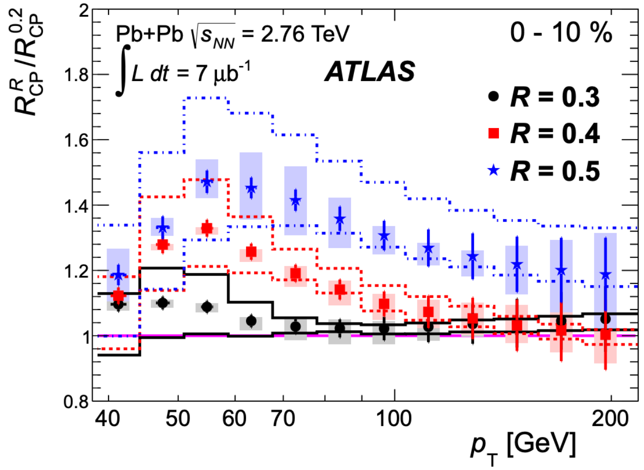

# Comparison across kinematic ranges

*STAR* Phys. Rev. C **102**, 054913

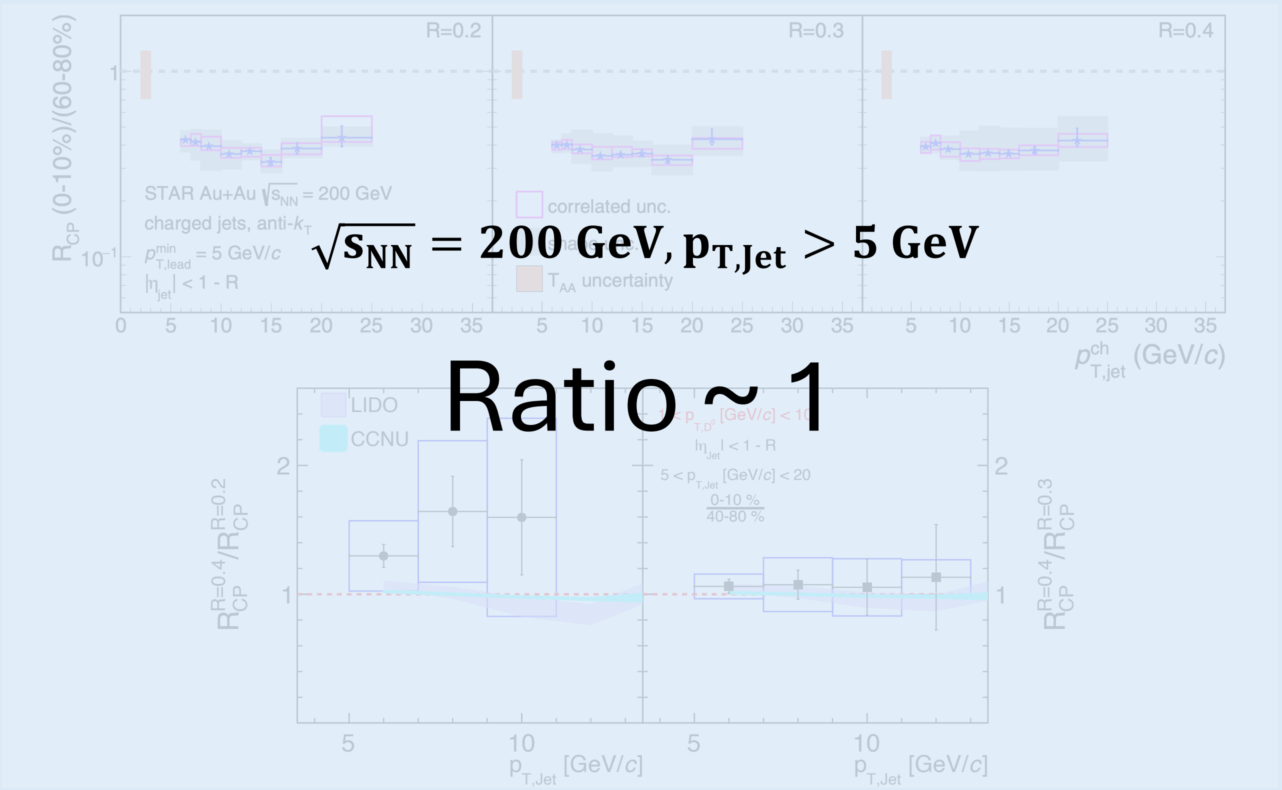


$\sqrt{s_{NN}} = 200\ \mathrm{GeV}, p_{T,Jet} > 5\ \mathrm{GeV}$

Ratio ~ 1

*ALICE* Phys. Let. B **849**, 138412

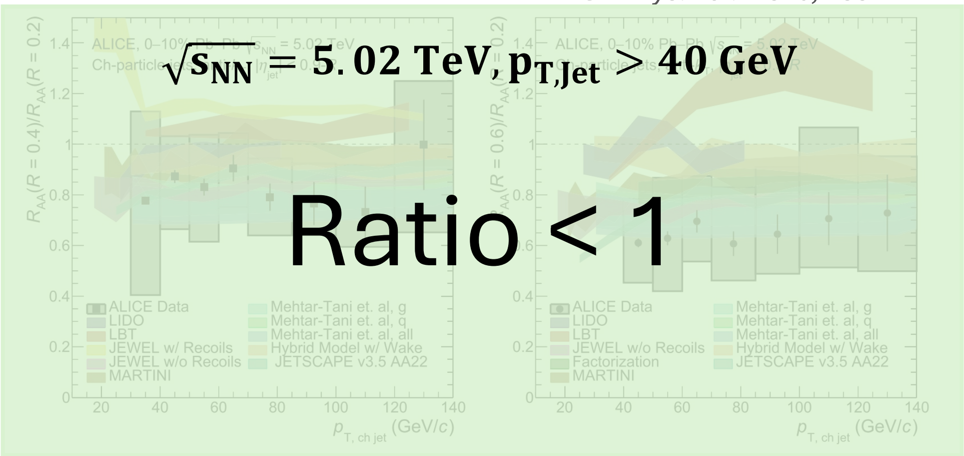


$\sqrt{s_{NN}} = 5.02\ \mathrm{TeV}, p_{T,Jet} > 40\ \mathrm{GeV}$

Ratio < 1

*ATLAS* Phys. Let. B *719*

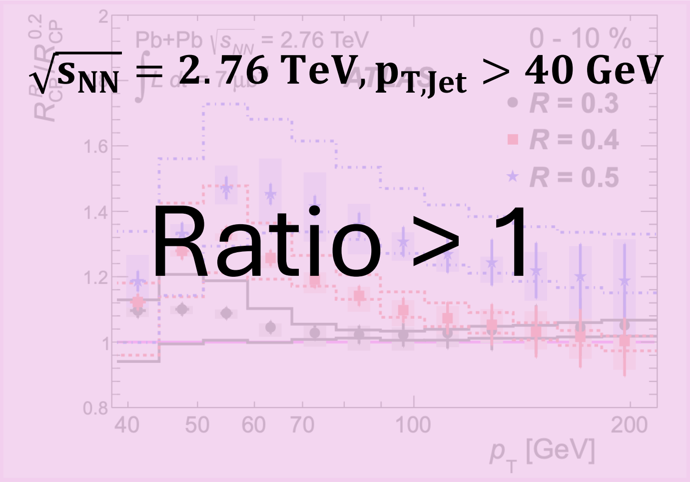


$\sqrt{s_{NN}} = 2.76\ \mathrm{TeV}, p_{T,Jet} > 40\ \mathrm{GeV}$

Ratio > 1

**Contradictory behaviors just due to different kinematic ranges (?)**

# Summary

- Exciting measurements for heavy flavor jets at STAR with $D^0$ meson tagged jets
- $D^0$ jet yield suppressed in central collisions, mainly for hard fragmented jets
- No radial profile modification for $D^0$ in jets in central Au + Au collisions
- Qualitative agreement with LIDO for radial profile, yield slightly underpredicted for central collisions

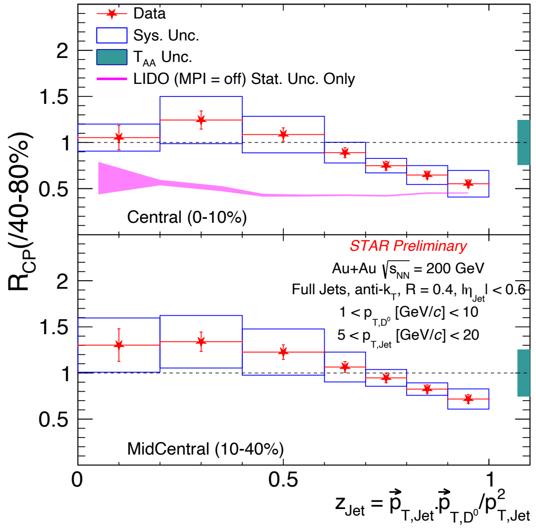


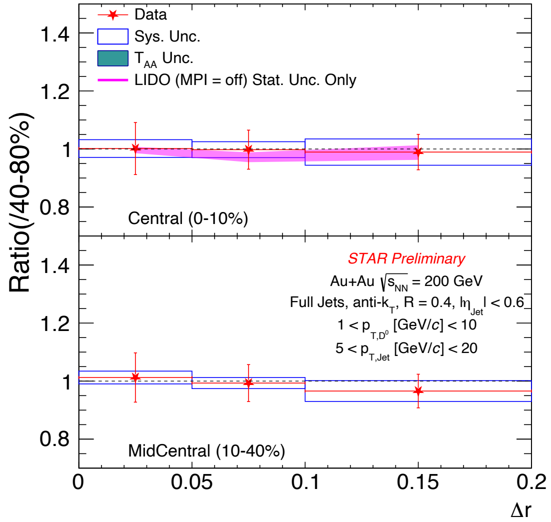

# Summary

- No jet cone size dependence observed for yield suppression in medium
- In agreement with models, and STAR's inclusive jet measurement
- Behavior across different kinematic ranges different – **different effects taking precedence?**

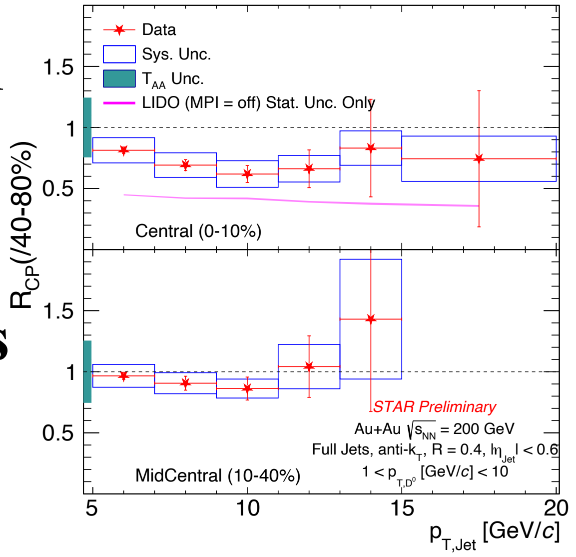


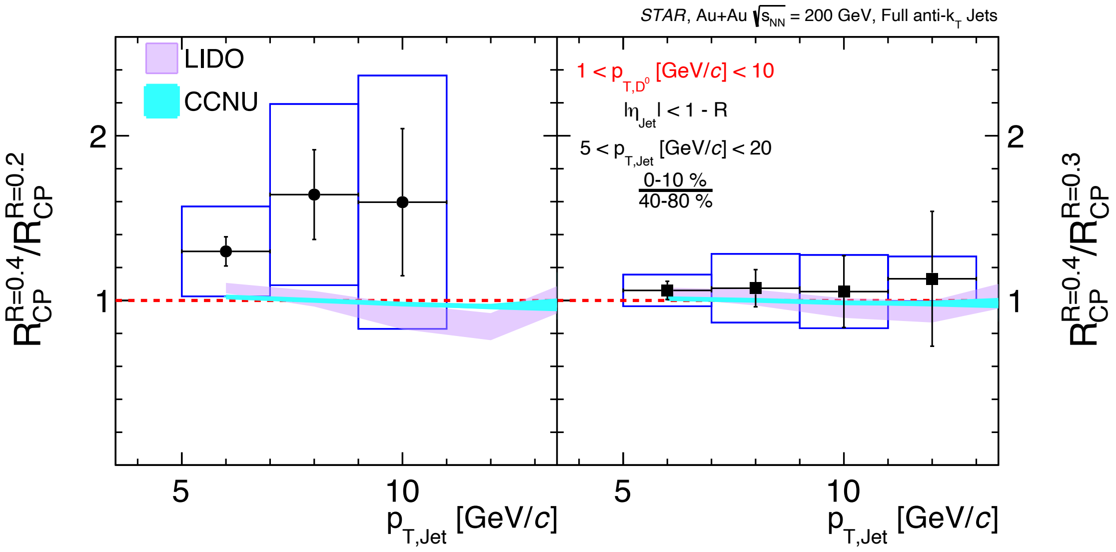

# What's next ?

$$\lambda_{\beta}^{\kappa} = \sum_{\text{const}\in\text{jet}} \overbrace{\left(\frac{p_{\text{T,const}}}{p_{\text{T,jet}}}\right)^{\kappa}}^{\text{soft/hard radiation}} \times \overbrace{r(\text{const},\text{jet})^{\beta}}^{\text{collinearity sensitive}}$$

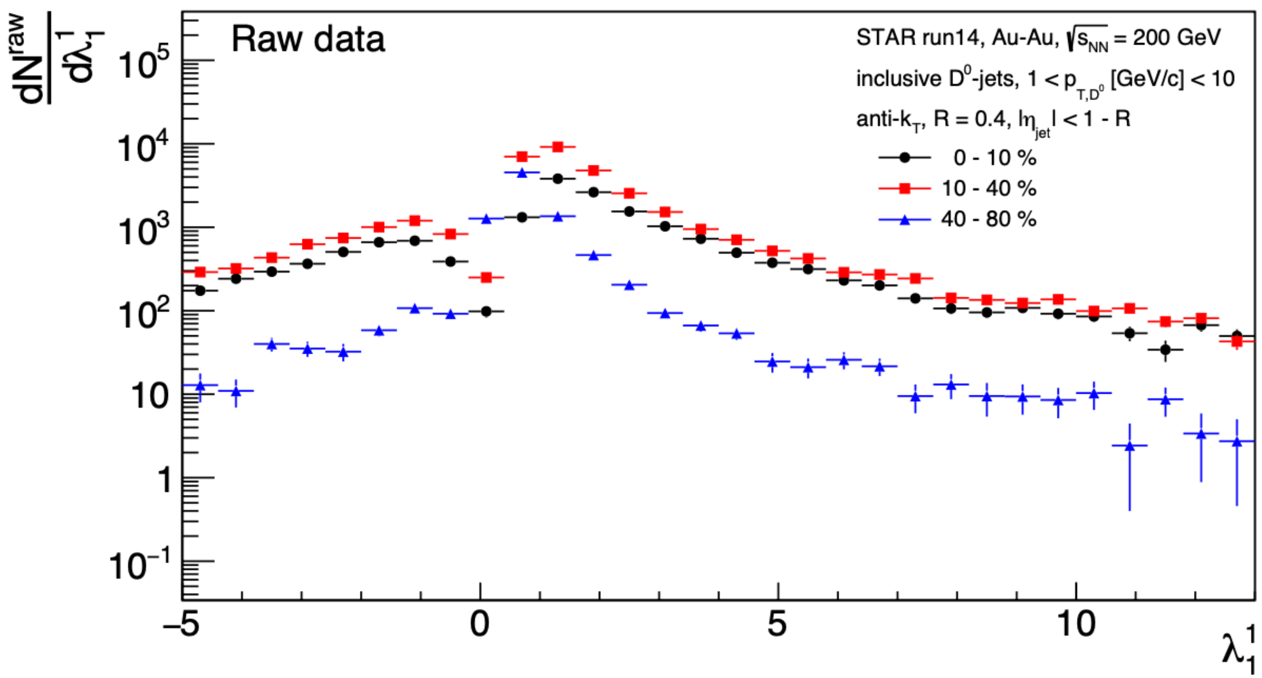


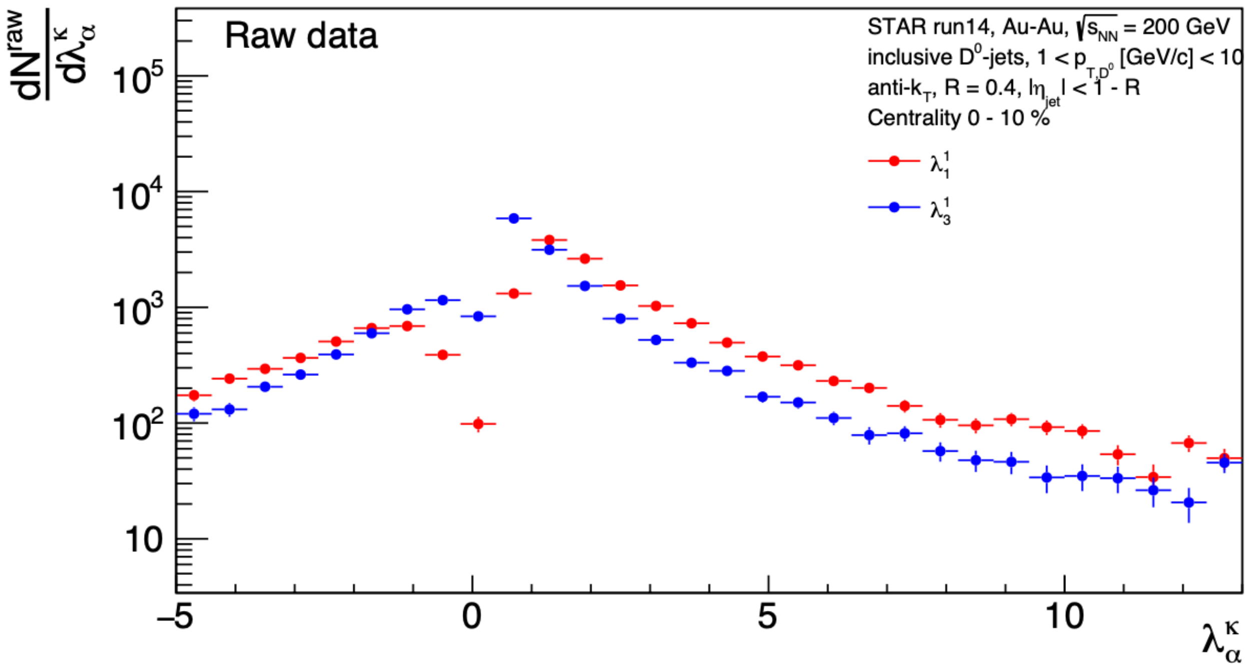


- Uncorrected angularities for $D^0$ tagged jets at STAR
- Ongoing effort to use multidimensional unfolding to correct for detector effects – incredibly challenging with background, even with newer tools like Multifold

# *Thank You*

# Summary

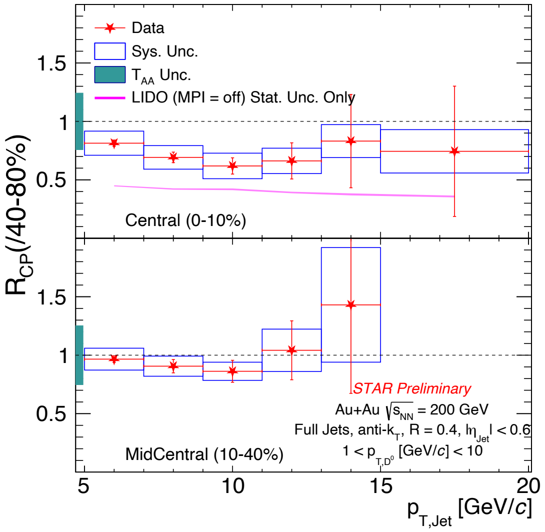

Data
Sys. Unc.
T_AA Unc.
LIDO (MPI = off) Stat. Unc. Only
Central (0-10%)
MidCentral (10-40%)
STAR Preliminary
Au+Au √s_NN = 200 GeV
Full Jets, anti-k_T, R = 0.4, |η_Jet| < 0.6
1 < p_T,D⁰ [GeV/c] < 10
R_CP(/40-80%)
p_T,Jet [GeV/c]


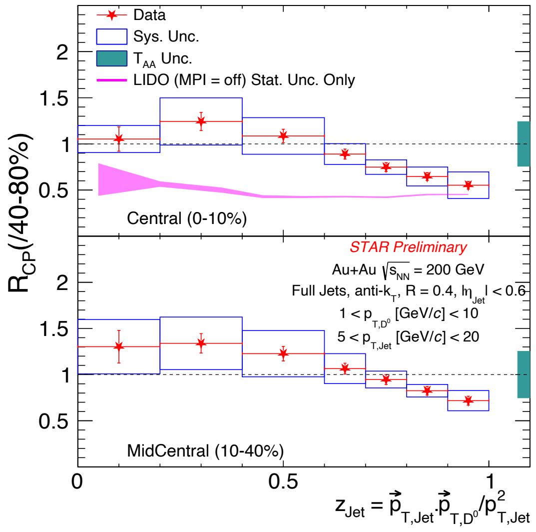

Data
Sys. Unc.
T_AA Unc.
LIDO (MPI = off) Stat. Unc. Only
Central (0-10%)
MidCentral (10-40%)
STAR Preliminary
Au+Au √s_NN = 200 GeV
Full Jets, anti-k_T, R = 0.4, |η_Jet| < 0.6
1 < p_T,D⁰ [GeV/c] < 10
5 < p_T,Jet [GeV/c] < 20
R_CP(/40-80%)
z_Jet = p_T,Jet.p_T,D⁰/p²_T,Jet


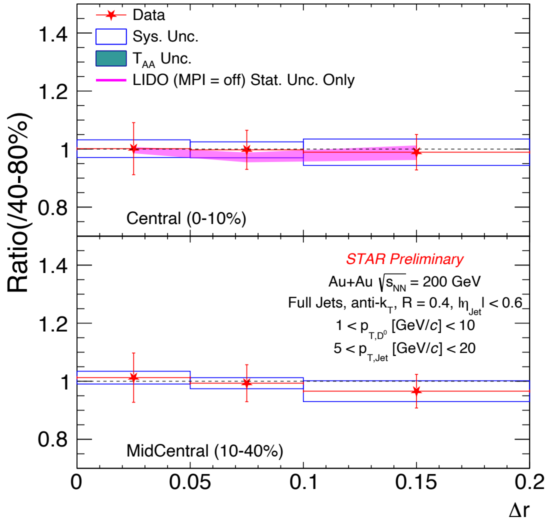

Data
Sys. Unc.
T_AA Unc.
LIDO (MPI = off) Stat. Unc. Only
Central (0-10%)
MidCentral (10-40%)
STAR Preliminary
Au+Au √s_NN = 200 GeV
Full Jets, anti-k_T, R = 0.4, |η_Jet| < 0.6
1 < p_T,D⁰ [GeV/c] < 10
5 < p_T,Jet [GeV/c] < 20
Ratio(/40-80%)
Δr


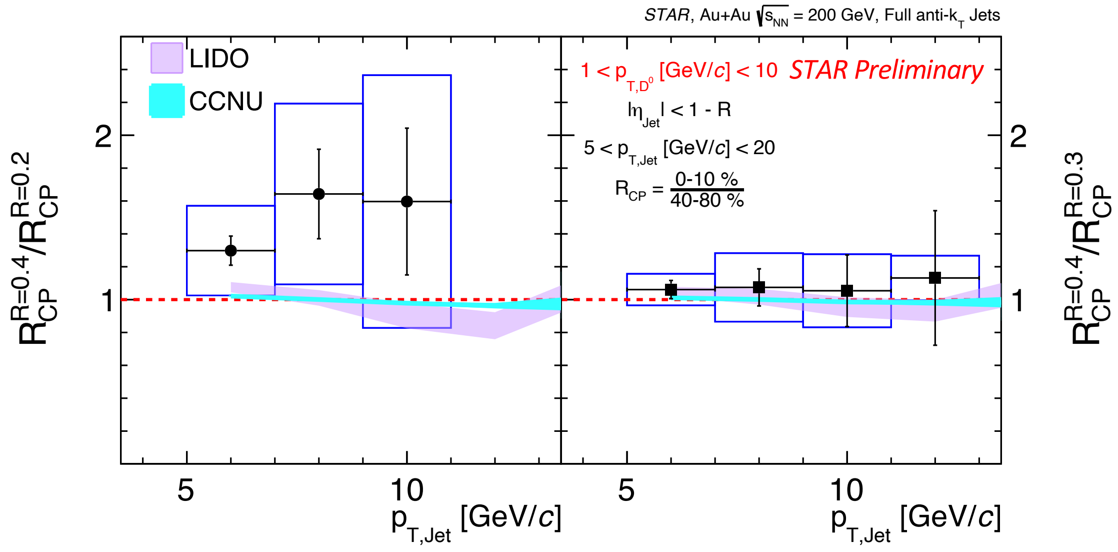

STAR, Au+Au √s_NN = 200 GeV, Full anti-k_T Jets
LIDO
CCNU
1 < p_T,D⁰ [GeV/c] < 10
STAR Preliminary
|η_Jet| < 1 - R
5 < p_T,Jet [GeV/c] < 20
R_CP = 0-10 % / 40-80 %
R_CP^R=0.4/R_CP^R=0.2
R_CP^R=0.4/R_CP^R=0.3
p_T,Jet [GeV/c]


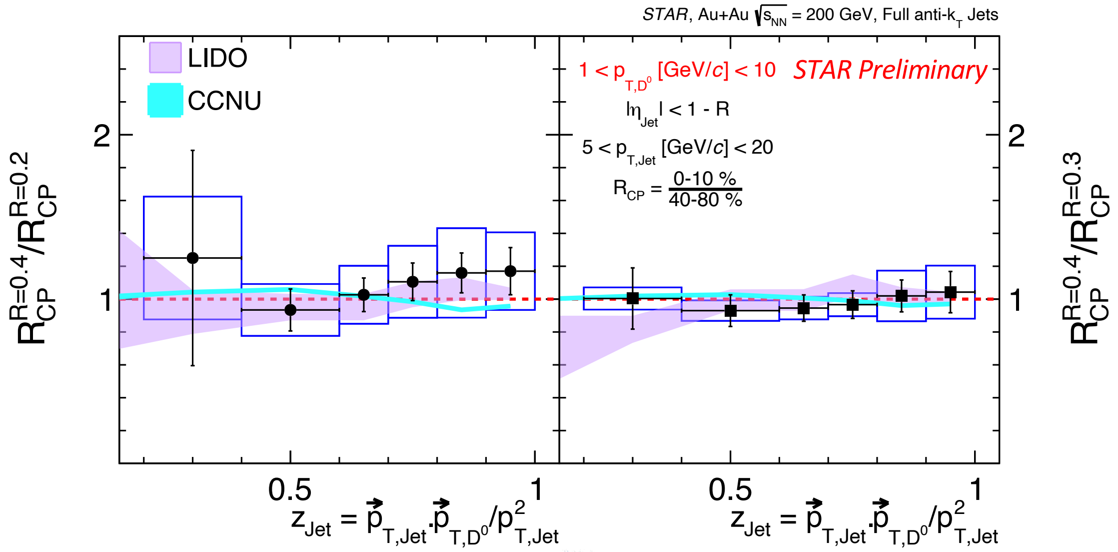

STAR, Au+Au √s_NN = 200 GeV, Full anti-k_T Jets
LIDO
CCNU
1 < p_T,D⁰ [GeV/c] < 10
STAR Preliminary
|η_Jet| < 1 - R
5 < p_T,Jet [GeV/c] < 20
R_CP = 0-10 % / 40-80 %
R_CP^R=0.4/R_CP^R=0.2
R_CP^R=0.4/R_CP^R=0.3
z_Jet = p_T,Jet.p_T,D⁰/p²_T,Jet

# Differential jet shape for heavy quark in vacuum

CMS, JHEP05 (2021) 054

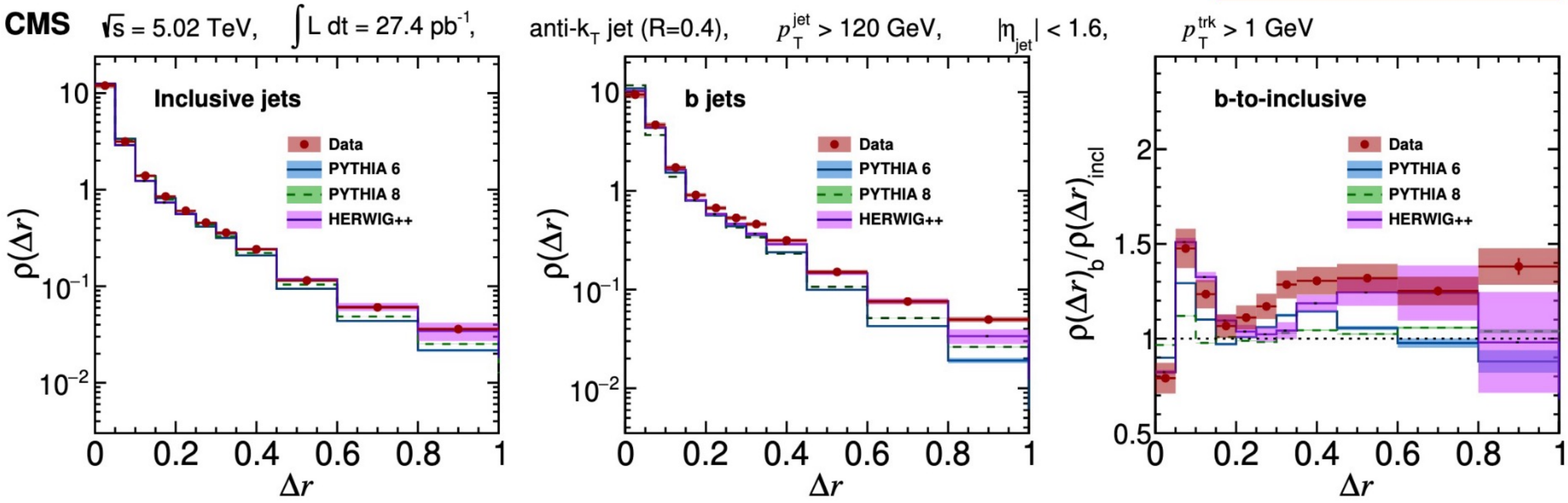


**Bottom quark jet (b-jets) shapes modified in vacuum, possibly due to dead cone**

# Fragmentation pattern for heavy quark

**CMS**, JHEP05 (2021) 054

**CMS**, pp $\sqrt{s}$ = 5.02 TeV

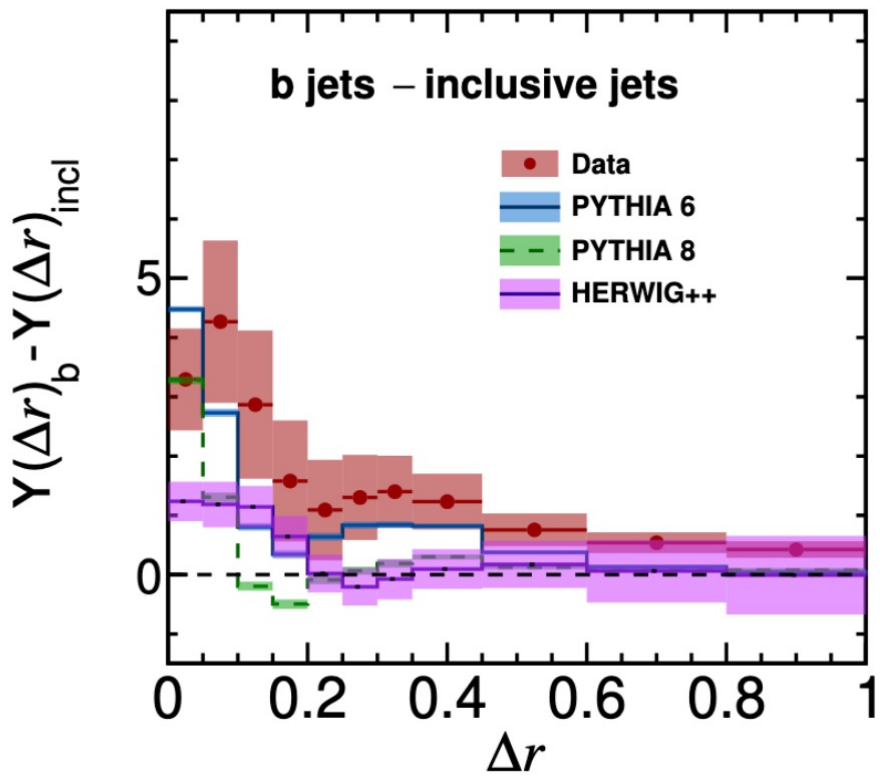


$$Y(\Delta r) = \frac{1}{N_{\text{jet}}} \frac{d^2 N_{\text{track}}}{d\Delta r \, dp_{\text{T,track}}}$$

**Higher yields of low $p_T$ charged-particle close to jet axis in b-Jets vs inclusive jets in vacuum**

*~ Different fragmentation pattern for heavy quarks*